PARAMETRIZATION OF RADIATION TRANSFER IN THE ECMWF MODEL

Jean-Jacques Morcrette
European Centre for Medium-range Weather Forecasts
Shinfield Park, Reading, U.K.

Abstract

The successive versions of the radiation transfer scheme used in the ECMWF operational model, including the version which became operational on 2 May 1989, are reviewed and their results are compared to results of more detailed radiation models made available thanks to the ICRCCM programme.

Results from the ECMWF model including the new radiation scheme indicate a greater overall sensitivity of the model to cloud-radiation interactions. Radiative cooling in the subtropics is increased. A decrease in radiative cooling in the higher layers of the tropics is caused by larger longwave impact of the high level clouds. An increase in the radiative energy available at the surface and an overall cooling of the troposphere generate larger turbulent heat fluxes. All these changes contribute to a higher level of convective activity, resulting in a more energetic hydrological cycle and a more active model with higher levels of zonal and eddy available potential energy and of eddy kinetic energy at all wave numbers. The warm bias in stratospheric temperature is greatly reduced. The divergence in the tropics is larger and does not weaken as much after a few days of integration as with the old operational radiation scheme, thus improving the Hadley circulation. The radiation budget at the top of the atmosphere (TOA) is now in good agreement with satellite observations.

Given the improved radiation fields at TOA, we also illustrate the potential of the "model-to-satellite" approach where pseudo satellite radiances are directly computed from the model temperature, humidity and cloudiness with the model's radiation scheme and compared to actual satellite measurements for validating the parametrization of the surface-cloud-radiation interactions.

1. INTRODUCTION

As radiation is the only source and ultimate sink of energy for the Earth's atmosphere system, the transfer of radiative energy within the Earth's atmosphere system is a process of the utmost importance for the climatic equilibrium of the Earth's atmosphere system, and previous studies (e.g., Fels and Kaplan, 1975; Ramanathan et al., 1983) have shown the large sensitivity of simulated model climates to the parametrization of the radiation transfer. On the contrary, radiation is usually thought to be a parameter of secondary importance for short term weather prediction. For long, it has been considered as sufficient to incorporate into models dedicated to numerical weather prediction (NWP) a much cruder representation of the radiative processes. In doing so, it is assumed that it is more important to get reasonable estimates of the vertical and horizontal gradients of the radiative cooling/heating (which are dominated by the three-dimensional cloud distribution) than to get accurate description of the clear-sky radiation fields.

However, at ECMWF, emphasis has always been put on medium-range weather forecasts, so that both accuracy and interactivity have been required from the radiation transfer scheme. Then, from 1979, the ECMWF cloud-radiation scheme has included features found in climate models only years later: cloud fractional cover, explicit calculation of the cloud reflectivity, transmissivity and absorptivity as a function of a diagnosed cloud liquid water content, radiatively active aerosols.

In a recent paper, Arpe (1988) analyzed the errors present in the current system (as of the beginning of 1988). They can be separated in three categories with regards to their relationships to potential deficiencies in the radiative transfer parametrization used in the model: first, those which clearly display the signature of a deficient cloud-radiation parametrization, such as the unrealistic smooth field of outgoing longwave radiation at the top of the atmosphere, the stratospheric warm temperature bias and the too small clear-sky radiative cooling in the tropics; second, those which are probably related to an improper three-dimensional distribution of the radiative forcing. Under this heading we find the presence of a negative bias in surface temperature at high latitudes in spring, the slowing down of the model hydrological cycle after 4 forecast days, and the small value of the maximum of the tropical divergence in the troposphere (600-300 hPa). Finally, the third category includes the

systematic errors that cannot be connected to weaknesses in the representation of cloud-radiation interactions, like, as in most large-scale numerical models of the atmosphere, a poleward and upward shift of the subtropical jets and excessive easterlies in the upper tropical troposphere.

Recently, the Intercomparison of Radiation Codes in Climate Models (ICRCCM) programme (Luther et al., 1988) has provided the opportunity to use the results of very detailed radiation models. They can be considered as state-of-the-art reference calculations, at least in a relative sense, for the much cruder parametrizations used in large-scale numerical models of the atmosphere. Such comparisons have been carried out for the ECMWF operational radiation scheme. They have shown the presence of a number of systematic errors, both in the longwave and shortwave radiation transfer parametrizations, in clear-sky as well as in cloudy atmospheres (Morcrette, 1990).

This paper, first, briefly documents the results of such comparisons done with the various operational versions of the ECMWF radiation scheme. The various changes undergone by the ECMWF radiation scheme are described in section 2 from a historical point of view and results of comparisons with more detailed models are presented. Section 3 then reports of an extensive study of the effects of a new radiation scheme which corrects most of the deficiencies of the previous operational radiation code. In those results, emphasis is made on the long-term response of the model. The new radiation scheme gives clear-sky radiation fields at the top of the atmosphere (TOA) in much better agreement with reference calculations and satellite measurements. Then pseudo-satellite radiances simulated from the model humidity, temperature and cloudiness can be directly compared to actual satellite measured radiances. Such comparisons are a powerful tool to validate model parametrizations of the surface-cloud-radiation interactions. Section 4 illustrates the potential of this "model-to-satellite" approach.

2. THE HISTORY OF RADIATION AND CLOUD PARAMETERIZATIONS AT ECMWF

Since the beginning of operational weather forecasting at the European Centre for Medium-range Weather Forecasts (ECMWF), the model has known so far only three versions of the radiation transfer scheme, hereafter referred to as EC1, EC2, and EC3.

The first one (EC1) was used from the first ever produced ECMWF operational 10-day forecast on 1 August 1979 till beginning of December

1984. The EC1 scheme was first used in the 15-level N48 grid-point model (Burridge and Haseler, 1979; Tiedtke et al., 1979), then from 21 April 1983 in the 16-level T63 spectral model (Simmons and Jarraud, 1984). Longwave cooling rates presented for EC1 in this section are displayed on this latter vertical grid which uses a hybrid coordinate resembling the sigma coordinate close to the ground, but reducing to a pressure coordinate at stratospheric levels. The high atmosphere is described by 6 levels at about 326, 251, 186, 128, 75 and 25 hPa.

The original ECMWF radiation scheme (Geleyn and Hollingsworth, 1979) deals with the interaction between line absorption and scattering using a photon path distribution method. Scattering by air molecules, cloud water droplets and aerosols which shows little dependence on wavelength is first treated via a two-stream approximation of the radiative transfer equation using spectrally averaged "grey" coefficients. Then the highly wavelength dependent gaseous absorption is accounted for by multiplying the "grey" fluxes (obtained for the previous pure scattering atmosphere) by the transmission function corresponding to the pathlengths of all photons contributing to the "grey" fluxes.

Transmission functions τ are evaluated in five spectral intervals (3 in the longwave and 2 in the shortwave) for each of the absorbers (water vapor, ozone and uniformly mixed gases - CO_2, CH_4, N_2O, CO and O_2 -) with the help of an empirical function (Geleyn, 1977) of u_r and u, the reduced and unreduced amounts of absorbers

$$- \ln \tau = \frac{a\,u}{\sqrt{1+bu^2/u_r}} + c\,u_r \qquad (1)$$

The term cu_r represents a continuum absorption. The coefficients a, b, and c incorporate the temperature dependence of the absorption (linearly dependent on 1 / T). They have been fitted to the experimental data of McClatchey et al. (1973) and Vigroux (1953). Two diffusivity factors are used to approximate the angular integration: 2 for the unreduced amount and 25/16 for the reduced amount of absorber. In the shortwave, the Rayleigh scattering effect is incorporated using empirical coefficients for which the effect of first scattering is well parametrized as a function of the solar zenith angle.

In the first version of the ECMWF radiation scheme, cloud cover is diagnosed as a function of relative humidity only (Geleyn et al., 1982) in all layers except in the well-mixed boundary layer where potential

temperature is lower than that at the surface for the layer in question and all layers underneath. Cloud radiative parameters (optical thickness, single scattering albedo and asymmetry factor) are derived from the experimental data of Zdunkowski et al. (1967). The optical thickness is related to the cloud liquid water path, assumed to be 0.2 percent of the saturated water vapor amount in the model layer. Operationally, vertically smoothed humidity profiles were used as inputs for this radiation scheme.

However, the photon path distribution method is valid provided that the gaseous absorption coefficient is infinitesimally small and there is only one source of radiation at the top of the atmosphere. These assumptions are not verified in the longwave domain and an "effective cooling-to-space approximation" was originally introduced by Geleyn and Hollingsworth (1979) to define a photon path length in clear-sky situations. Various studies (Slingo, 1982; Tanre et al., 1983; Morcrette and Geleyn, 1985) showed that this last approximation introduces an exaggerated sensitivity to small amounts of scatterer. In other respects, this implementation of the radiation transfer equation only allows the effect of the p-type H_2O continuum absorption to be included, without provision for that of the e-type absorption (Slingo, 1982).

A revised version of the longwave scheme (EC2) (but no change in the clear-sky shortwave parametrization nor in the model cloud optical parameters) was then developed which directly incorporates gaseous absorption in the solution of the two-stream equation (Ritter, 1984; Slingo and Ritter, 1985; Slingo et al., 1988) by using the technique of exponential sum fitting of the band transmission function (Wiscombe and Evans, 1977). This formulation allows full account of the H_2O continuum absorption to be taken (both e- and p-type components). On 4 December 1984, the revised version (EC2) became operational in the forecast model. However, the large humidity found in the planetary boundary layer in the ECMWF model operational at that time would have led to excessive PBL radiative cooling in the tropics with the full EC2 scheme, and the e-type continuum absorption was set to zero in the operational radiation scheme from pragmatic considerations.

In EC2, 5 spectral intervals are used to describe the longwave spectrum. In these intervals, the transmission functions are evaluated as sums of exponentials whose coefficients are derived from the 1980 version of the AFGL line parameter compilation (McClatchey et al., 1973; Rothman, 1981). Temperature and pressure dependence of the absorption is dealt with

using one-parameter scaled amounts of absorbers following the approach used in the LOWTRAN model (Selby and McClatchey, 1972).

On 1 May 1985, the ECMWF model underwent a major revision: The horizontal resolution went from a T63 to a T106 spectral representation, and various changes were introduced into the representation of the physical processes (Tiedtke et al., 1988; Slingo et al., 1988): Among them, (i) a shallow convection parametrization was added to the large-scale condensation and deep convection parametrizations which contributed to transport the excessive PBL moisture higher up in the atmosphere; (ii) the diagnostic formulation of the cloud cover relying simply on relative humidity (Geleyn et al., 1982) was replaced by a new diagnostic scheme (Slingo, 1987) using relative humidity, convective precipitation, vertical velocity and the gradient of potential temperature in the planetary boundary layer as predictors of the various levels of cloudiness. Simultaneously, the proportionality factor linking the cloud liquid water content (LWC) to the saturation mixing ratio of the layer where a cloud is diagnosed was increased to 1 percent to be consistent with the new distribution of fractional cloud cover.

On 13 May 1986, the vertical resolution was increased to 19 levels, with three new levels in the stratosphere. The high atmosphere is now described by 9 levels at about 326, 253, 191, 142, 103, 74, 50, 30 and 10 hPa. Longwave cooling rates presented for EC2 in section 3 are displayed on this presently operational vertical grid.

More recently, an extensive validation of the ECMWF radiation scheme was carried out, partly through comparisons with results of detailed models made available through the ICRCCM programme, partly through comparisons of model-generated radiation fields at the top of the atmosphere with well calibrated radiances measured by the Earth Radiation Budget Experiment (ERBE) (Morcrette and Fouquart, 1988). The presence of a number of systematic errors (that will be briefly discussed in the following) have led to the development of a new radiation scheme for the ECMWF model (Morcrette, 1990).

This new radiation package (EC3), which includes major changes in both shortwave and longwave radiation parametrizations and in the cloud optical properties assigned to the clouds, is based on an updated/revised version of the radiation schemes developed at the University of Lille (Fouquart and Bonnel, 1980; Morcrette and Fouquart, 1986; Morcrette et al., 1986; Frouin et al., 1988). Its main features are summarized in Table 1.

Table 1: Summary of the ECMWF new radiation code (EC3)

a. Clear-sky

(i) Shortwave: Two-stream formulation employed together with photon path distribution method (Fouquart and Bonnel, 1980) in 2 spectral intervals (0.25-0.68 and 0.68-4.0 μm).

Rayleigh scattering	Parametric expression of the Rayleigh optical thickness
Aerosol scattering and absorption	Mie parameters for 5 types of aerosols based on climatological models (WMO-ICSU, 1984).
Gas absorption	from AFGL 1982 compilation of line parameters
H_2O	1 interval
Uniformly mixed gases	1 interval
O_3	2 intervals

(ii) Longwave: Broad band flux emissivity method with 6 intervals covering the spectrum between 0 and 2620 cm^{-1}. Temperature and pressure dependence of absorption following Morcrette et al. (1986). Absorption coefficients fitted from AFGL 1982.

H_2O	6 spectral intervals, e- and p-type continuum absorption included between 350 and 1250 cm^{-1}
CO_2	Overlap between 500 and 1250 cm^{-1} in 3 intervals by multiplication of transmission
O_3	Overlap between 970 and 1110 cm^{-1}
Aerosols	Absorption effects using an emissivity formulation

b. Cloudy sky

(i) Shortwave

Droplet absorption and scattering	Employs a delta-Eddington method with τ and ω determined from LWP, and preset g and r_e
Gas absorption	Included separately through the photon path distribution method

(ii) Longwave

Scattering	Neglected
Droplet absorption	From LWP using an emissivity formulation
Gas absorption	as in (a.ii)

Timing: 8 ms for a grid-point calculation with the 19-level model on a CRAY-XMP48

The EC3 radiation scheme has evolved from narrow-band models with high spectral resolution (225 spectral intervals in the longwave, 208 in the shortwave) that were as much as possible compared to line-by-line calculations (Scott and Chédin, 1981) and in situ measurements. These detailed models were then degraded by introducing simplifying assumptions making them more computationally efficient. In that process, the sensitivity of the outputs (fluxes and heating/cooling rates) to the various assumptions have been monitored (Morcrette and Fouquart, 1985; 1986). In the longwave, those studies showed that one of the causes for major systematic errors is the use of wide spectral intervals which tend to overestimate the effects of the strong lines, thus giving a poor representation of the temperature and pressure dependence of the absorption.

In EC3, clear-sky longwave fluxes are evaluated with an emissivity method incorporating a parametrization giving a correct representation of the temperature and pressure dependence of the absorption (Morcrette et al., 1986). Clouds are introduced as grey bodies with a longwave emissivity depending on the cloud liquid water path following Stephens (1978).

Shortwave fluxes are computed using a photon path distribution method to separate the contributions of scattering and absorption processes to the radiative transfer. Scattering is treated with a Delta-Eddington approximation. Transmission functions are developed as Padé approximants. Coefficients for the molecular absorption are calculated from the 1982 version of the AFGL line parameters compilation. Cloud shortwave radiative parameters are the optical thickness and single scattering albedo linked to the cloud liquid water path, and a prescribed asymmetry factor (Fouquart, 1987). In EC3, a distinction is made between various cloud types by defining the optical thickness as a function not only of the liquid water path in the cloud but also of the effective radius r_e of the cloud particles, with r_e varying with height from 5 μm in the planetary boundary layer to 40 μm at 100 hPa. This last feature is an empirical attempt at dealing with the variation of cloud type with height, as smaller water droplets are observed in low-level stratiform clouds whereas larger particles are found in cumuliform and cirriform clouds. This radiation scheme has already been extensively tested in the ECMWF model (Morcrette, 1989a) and was introduced in the operational forecast model on 2 May 1989.

A list of publications reporting studies performed with the ECMWF

forecast model is available from ECMWF. As the operational scheme at the time of the experiments, EC1 is used in the cloud-radiation-oriented experiments discussed by Geleyn (1981), Cubasch (1981), Geleyn et al. (1982), Morcrette and Geleyn (1985), whereas EC2 is used in the studies reported by Slingo (1987), Slingo et al. (1988), Tiedtke et al. (1988).

Figure 1a presents the clear-sky cooling rate profile in a standard mid-latitude summer atmosphere computed by the various versions of the ECMWF radiation scheme and the results of the GFDL longwave line-by-line model (kindly provided by Dr. Fels). Similarly, Figure 1b compares the clear-sky heating rate profile in the same atmosphere computed by the ECMWF radiation codes and the detailed shortwave narrow-band model of Fouquart and Bonnel (1989). Concentrating on the last two versions of the ECMWF radiation code (EC2 and EC3), both figures show the large departures of EC2 with respect to the detailed models. They are as large as 0.70 K/day in the longwave, corresponding to a 10-15 percent underestimation of the longwave atmospheric absorption and as large as 0.50 K/day in the shortwave, corresponding to a 15-20 percent overestimation of the shortwave atmospheric absorption. Figures 1 also display a much better agreement of EC3 with these "reference" models (maximum errors in longwave and shortwave heating rates are 0.15 and 0.10 K/day respectively corresponding to a better than 5 percent agreement on both longwave and shortwave atmospheric absorptions). Such differences also translate into differences in clear-sky fluxes at the surface and TOA as seen in Tables 2 and 3: EC2 underestimates shortwave fluxes by 3 to 15 percent and longwave fluxes by about 5 percent, whereas fluxes computed with EC3 agree within 2 percent with those computed by the detailed models. More extensive comparisons of both the operational and the new radiation schemes with detailed radiation models were carried out for various clear-sky and cloudy standard atmospheres in the framework of the ICRCCM programme. Full results can be found in Morcrette (1990).

The new radiation scheme gives clear-sky fluxes in good agreement with detailed radiation models in both the shortwave and longwave parts of the spectrum. The revised cloud optical properties and increased cloud LWC give a much better agreement of the radiation fields produced by EC3 with the satellite observations.

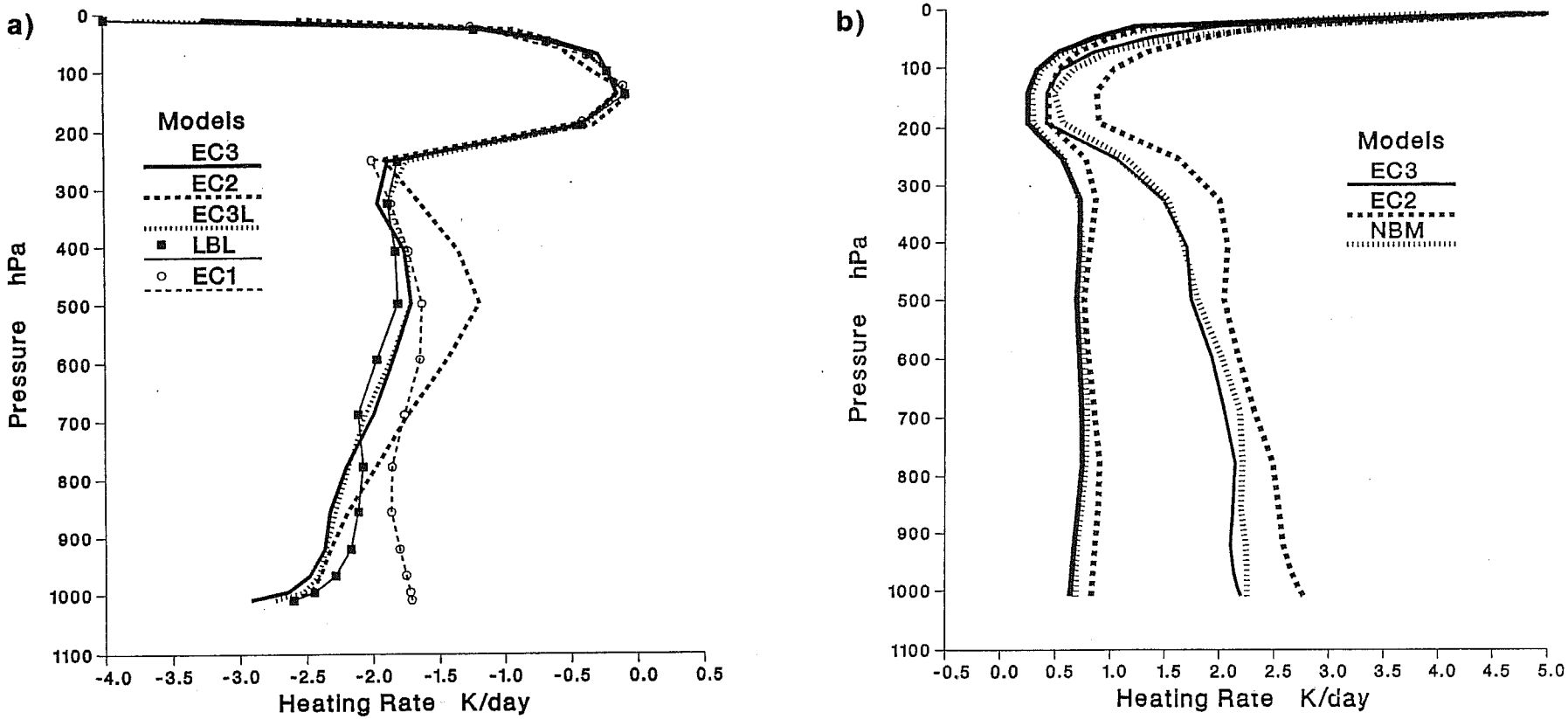

Fig. 1 Comparison of longwave (Fig. 1a) and shortwave (Fig. 1b) radiative heating rate profiles in a mid-latitude summer clear-sky standard atmospheres.

Fig. 1a EC1, EC2 and EC3 are the results of the various versions of the ECMWF longwave radiation parametrization on the ECMWF model vertical grid. LBL (dotted line) refer to the results of the GFDL line-by-line model; EC3L are results of the EC3 version but on the same vertical grid as LBL.

Fig. 1b NBM (dotted line) is the narrow-band model of Fouquart and Bonnel (1988), EC2 and EC3 correspond to the two versions of the ECMWF shortwave radiation parametrization. Results are presented for a surface albedo A_S = 0.2 and for 2 solar zenith angles, 30° and 75°.

Table 2: Net longwave fluxes at the top of the atmosphere, the tropopause level, and at the surface. Results in W m^{-2} are presented for 3 standard atmospheres and for various radiation models: LbL are the results of the GFDL line-by-line model; EC1, EC2, and EC3 refer to the various versions of the ECMWF longwave radiation parameterization. ECn calculations are performed on the ECMWF model vertical grid; EC3L are results of the EC3 version but on the same vertical grid as LbL.

	Top F^{net}				
	LBL	EC1	EC2	EC3	EC3L
TRO	298.3	266.7	282.5	302.9	300.5
MLS	289.0	263.1	273.7	292.3	291.0
SAW	203.0	186.0	194.5	204.0	203.2

	Tropopause F^{net}				
	LBL	EC1	EC2	EC3	EC3L
TRO	288.1	264.8	276.4	294.3	290.2
MLS	272.8	261.0	260.9	277.2	275.0
SAW	178.2	154.8	175.4	185.0	180.7

	Surface F^{net}				
	LBL	EC1	EC2	EC3	EC3L
TRO	66.5	67.9	85.1	72.3	72.5
MLS	79.1	69.1	90.5	84.1	83.8
SAW	82.9	64.2	82.0	85.4	84.1

3. IMPACT OF THE NEW RADIATION SCHEME ON THE ECMWF MODEL

This section reviews the most important results of an extensive study of the effects of the EC3 new radiation scheme which corrects most of the deficiencies of the previous operational radiation code (EC2). More detailed results of the comparisons can be found in Morcrette (1989a). In the following, comparisons are presented of two sets of experiments, hereafter referred to as OPE and NEW, respectively. The first includes the control integrations performed with the operational ECMWF forecast model (until the end of April 1989, i.e., EC2). The second set consists of integrations performed with the same model, but with the new radiation scheme (EC3).

The new scheme differs from the operational scheme through:

(i) a smaller shortwave H_2O absorptivity, which reduces the clear-sky shortwave heating and increases the downward solar radiation at the surface;

Table 3: Comparison of shortwave radiation fluxes at the surface, tropapause, and top of the atmosphere, for clear-sky standard tropical, mid-latitude summer and sub-arctic winter atmospheres, for various values of the solar zenith angle ϑ and of the surface albedo A_s.
All fluxes are in W m^{-2}.

	DNSUR	NTTRO	UPTOA	ABTOT
TRO, $\vartheta = 30^o$, $A_s = 0.2$				
NBM	917.1	937.2	209.5	235.0
EC2	861.6	933.7	208.1	280.8
EC3	931.0	937.6	210.4	223.2
MLS, $\vartheta = 30^o$, $A_s = 0.2$				
NBM	930.6	928.7	211.5	222.1
EC2	876.7	920.6	210.2	266.5
EC3	940.9	928.8	211.1	214.3
MLS, $\vartheta = 75^o$, $A_s = 0.2$				
NBM	230.4	254.6	77.3	90.5
EC2	201.7	243.9	84.4	106.4
EC3	237.6	257.2	74.0	88.0
MLS, $\vartheta = 30^o$, $A_s = 0.8$				
NBM	969.6	410.1	722.5	261.8
EC2	944.7	434.6	684.2	304.4
EC3	995.8	401.9	729.5	249.5
MLS, $\vartheta = 75^o$, $A_s = 0.8$				
NBM	239.1	122.6	207.7	96.6
EC2	217.0	128.1	197.5	111.3
EC3	247.9	120.5	209.0	93.6
SAW, $\vartheta = 75^o$, $A_s = 0.8$				
NBM	261.3	96.0	224.7	75.1
EC2	245.9	98.6	221.1	81.8
EC3	269.2	97.4	226.0	72.3

(ii) an improved temperature and pressure dependence of the longwave absorption, which increases the longwave cooling in mid-troposphere and stratosphere. It corrects the underestimation of the clear-sky outgoing longwave radiation (OLR) at the top of the atmosphere shown by the operational radiation scheme.

(iii) the presence of both the e- and p- type components of the H_2O continuum absorption, which cools the tropical planetary boundary layer

(PBL) (only p-type absorption is accounted for in the operational scheme),

(iv) cloud optical properties derived from a more realistic model cloud. As documented in Morcrette (1990), the operational radiation scheme uses cloud optical properties derived from a model cloud, which is a radiation fog (Zdunkowski et al., 1967) with a fairly narrow drop size distribution around an effective radius of 2.25 μm. Such a cloud is quite an efficient scatterer already at small LWPs. Therefore relatively small cloud LWPs ensure a reasonable description of the net shortwave radiation at the top of the atmosphere. On the contrary, for small LWPs (such as those corresponding to the higher-level clouds), the longwave emissivity is quite low. This, together with the underestimation of the clear-sky outgoing longwave flux, explains the lack of contrast in OLR produced by OPE.

(v) a diagnostic formulation of the cloud liquid water content independent of the model's vertical grid. This usually increases the liquid water content (LWC) of the diagnosed layer clouds in NEW integrations compared to OPE integrations.

3.1. Global budgets

Both the energy and hydrological cycles are affected by the change of radiation scheme. They are intensified by about 20 and 15 percent respectively, as is evident from the global mean values of net radiative cooling and net heating by convection, large-scale condensation and surface heat fluxes (Fig. 2), and from the values of precipitation and surface evaporation (Fig. 3). When compared to the climate estimates of Hoyt (1976), the new radiation scheme produces too high values of the energy balance (NEW: 111 W m^{-2} ; OPE: 86 W m^{-2}), with similar results for the hydrological cycle compared to Jaeger's (1976) climatology. However, the more recent climatology of Verstraete and Dickinson (1986) indicates higher values at 105 W m^{-2} for the mean annual atmospheric energy budget.

In the early stages of the forecasts, an intense spin-up of the hydrological budget shows up as a large imbalance between the moisture supply by surface evaporation and the loss due to precipitation. The result is that the model dries during the forecast. The new radiation scheme does not improve that aspect. Furthermore, as all the experiments presented in this paper have been run from initial conditions analysed with the model including the operational radiation scheme, there is an even bigger spin-up in the NEW experiments.

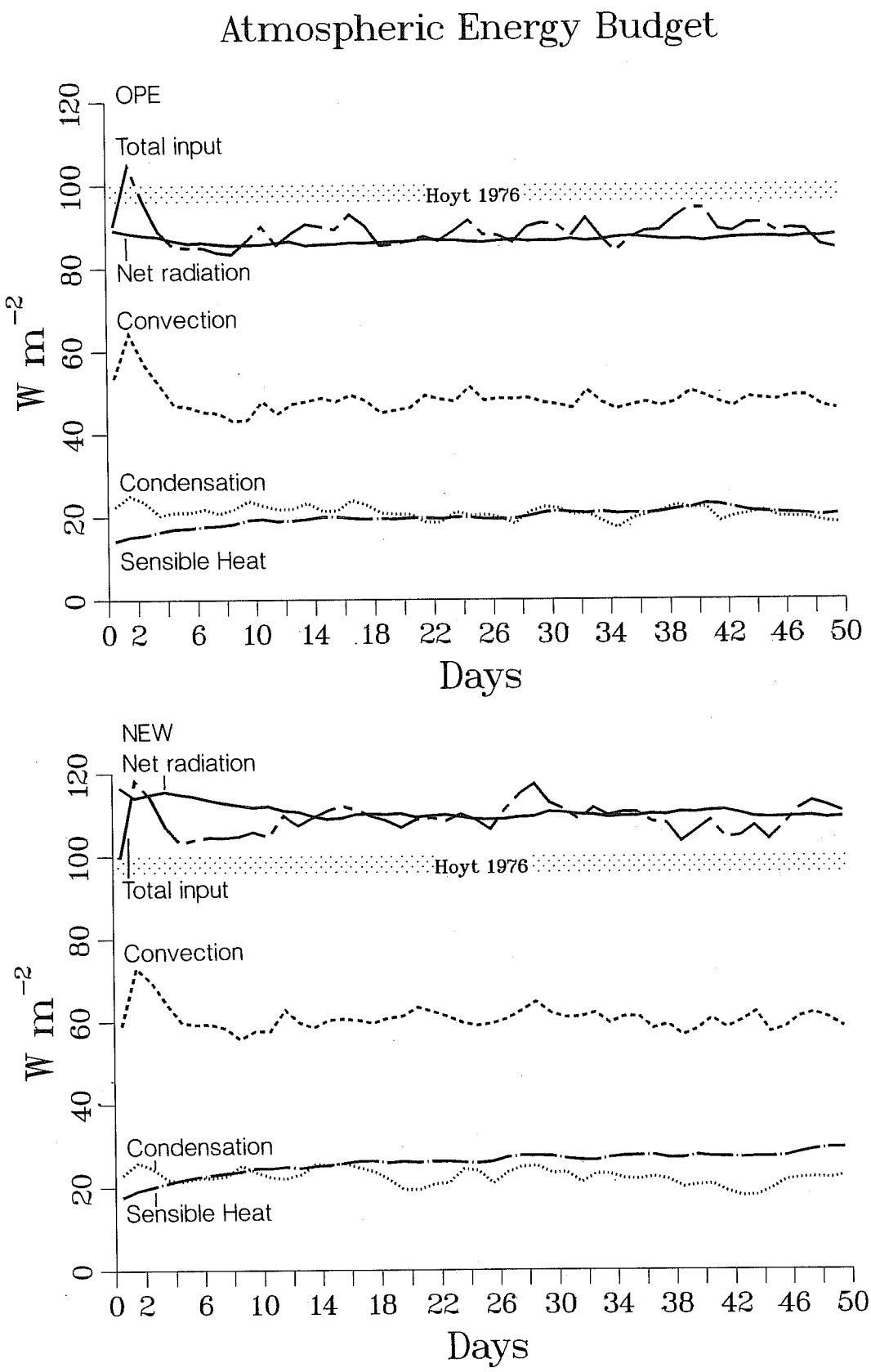

Fig. 2 Time evolution of diabatic heating due to radiation, cumulus convection, large-scale condensation and turbulent heat transfer for the whole globe in operational forecast (top) and forecast with new radiation scheme (bottom). Initial date is 01/06/87.12Z. Results are for the first 50 days of T42 90-day integrations. Climatological data from van Hoyt (1976).

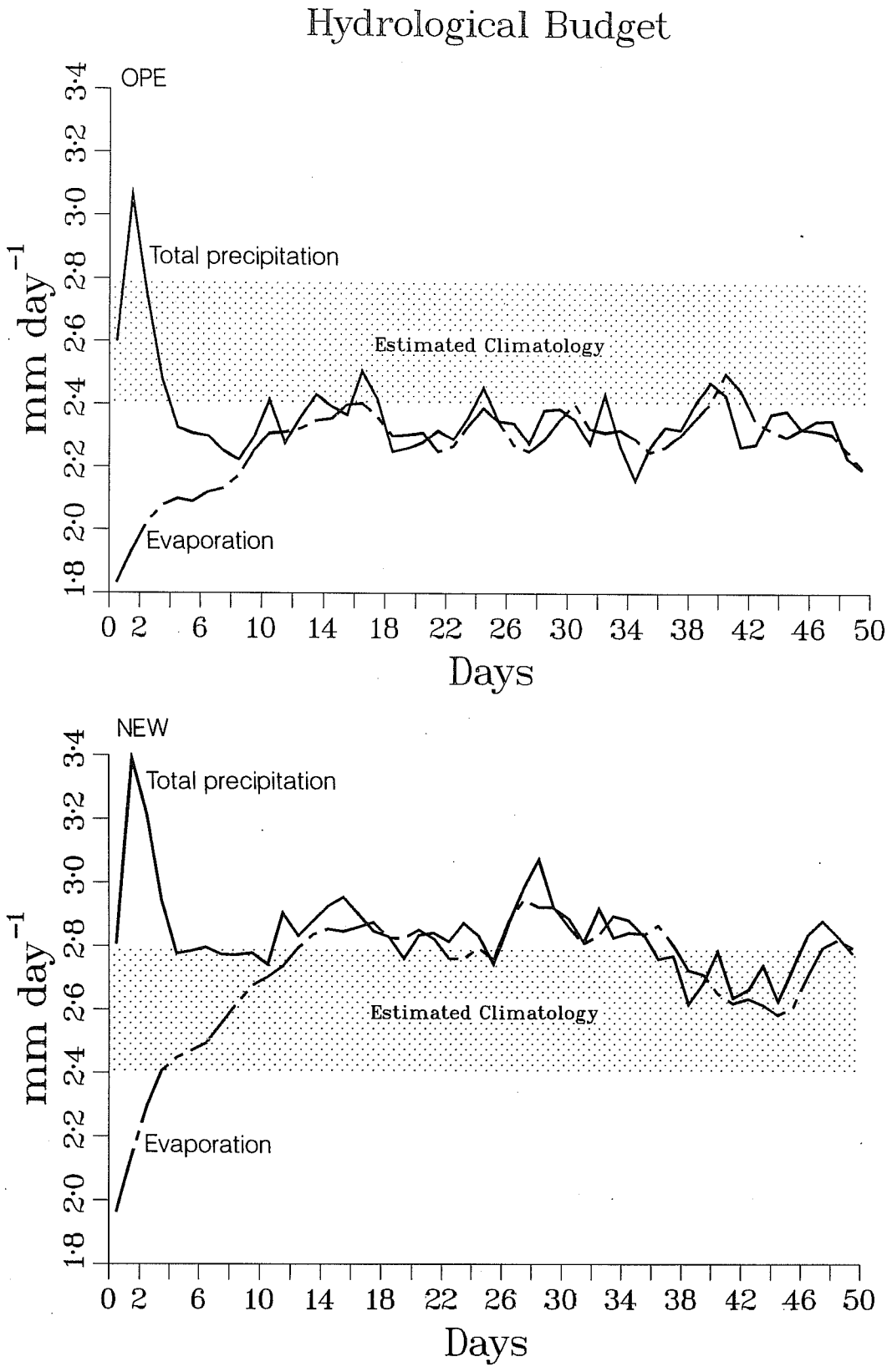

Fig. 3 As in Fig. 2, but for total precipitation and surface evaporation. Climatological data are from Jaeger (1976).

Figure 2 shows that, after the initial adjustment period, the atmospheric energy budget is increased through increase in cumulus convection (by about 25 percent, from 47 to 60 W m^{-2} for the displayed experiments) and in surface sensible heat (by about 30 percent, from 20 to 26 W m^{-2}) with a rather constant contribution from large-scale condensation (20 W m^{-2}). The surface energy budget, shown in Figure 4 is also increased (by about 10 percent, from 162 to 177 W m^{-2}). The change of radiation scheme gives an increased input of solar radiation (by about 12 percent, from 160 to 180 W m^{-2}) and a decreased output of terrestrial radiation (by about 10 percent, from 75 to 67 W m^{-2}). As the model sea surface temperature (SST) is specified, only the land surface can adjust to a larger radiative input. The increased global latent and sensible heat fluxes (by 20 and 30 percent, from 68 to 80 W m^{-2}, and from 20 to 26 W m^{-2}, respectively) mainly reflect the cooling of the lower troposphere by NEW.

To put the previous results in perspective, we first consider the magnitude of the change that the new radiation scheme has caused in the global energy balance of the model. The main difference between NEW and OPE is seen for the solar radiation absorbed by the atmosphere (from 85 to 66 W m^{-2}). The decrease in clear-sky shortwave absorption is seen in global mean values indicating that the presence of clouds (which varies from 0.488 in OPE to 0.508 in NEW) has not substantially modified the forcing (a decrease of about 20 percent of the clear-sky shortwave absorption); on the opposite, the increase in clear-sky longwave cooling (of about 12 percent, seen in instantaneous one-dimensional calculations) is partly compensated by the heating below the more radiatively active high-level cloudiness in the tropics and the atmospheric loss by longwave radiation only increases from 171 to 177 W $^{-2}$. At the surface, the net total radiation increases from 87 to 117 W m^{-2}. The change of radiation scheme thus has a large impact: the overall net atmospheric cooling changes by more than 30 percent from 86 to 116 W m^{-2} from 0.74 to 0.95 K day^{-1}.

This effect is even larger in the tropics. There, the mean annual net heating of about 60 W m^{-2} is the sum of a 320 W m^{-2} heating by absorption of solar radiation and a 260 W m^{-2}cooling by longwave emission. The main point, stressed by Ramanathan (1986) is that this net heating of only about 20 percent of the absorbed solar radiation (with the remaining 80 percent heating the tropical surface) is the driving force for the general circulation of the atmosphere and the ocean. Therefore, a change of 10 percent in the column absorbed solar radiation or in the longwave emission

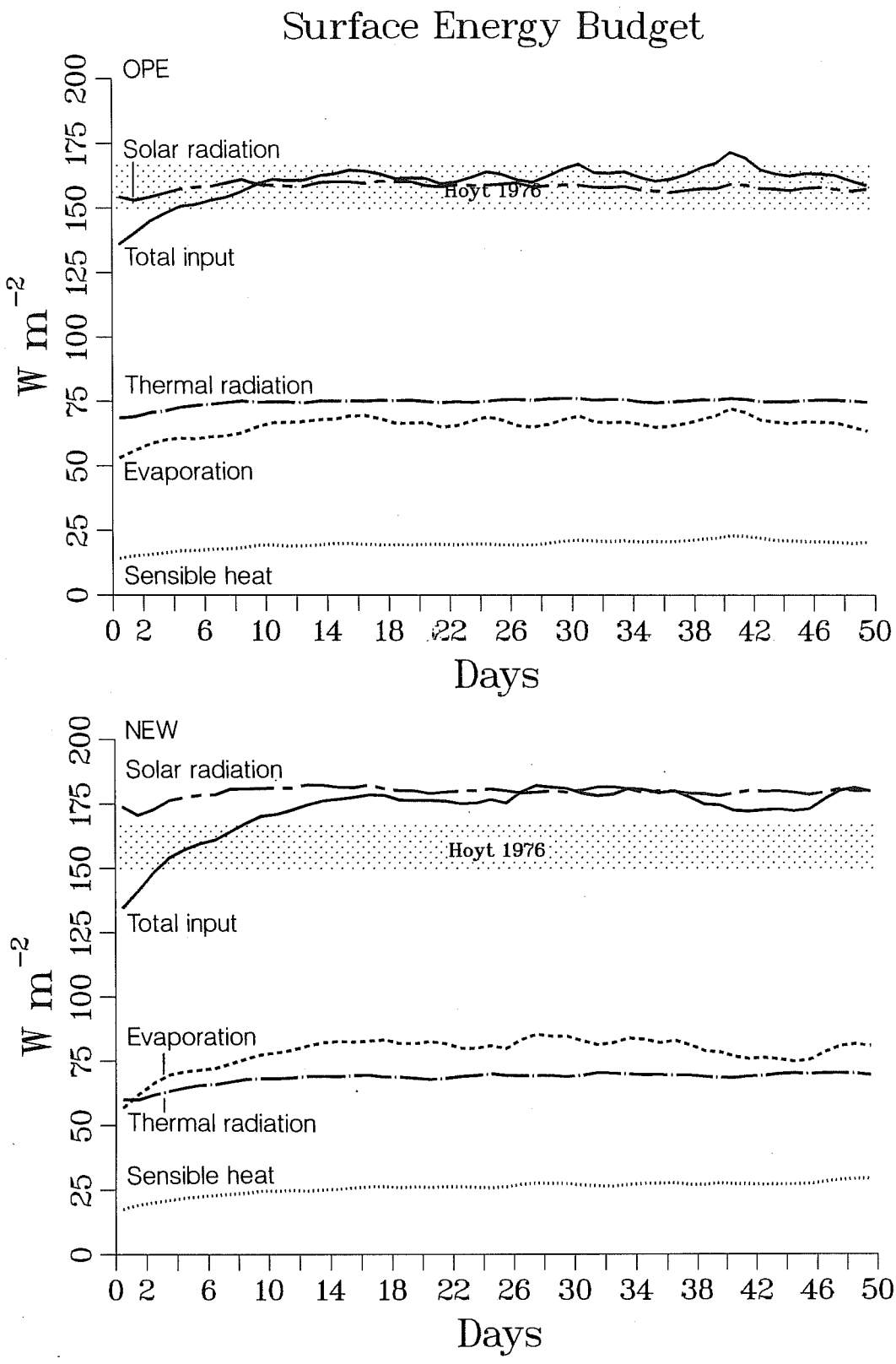

Fig. 4 As in Fig. 2, but for the components of the surface energy budget, namely net solar radiation, net thermal radiation, sensible and latent heat fluxes. Climatological data from van Hoyt (1976).

may potentially translate into a factor of five times larger change (i.e., 50 percent) in that driving force or likewise in the required poleward transport of heat.

Also, as a whole, the troposphere is subject to a net radiative cooling (of about 100 W m^{-2}) whereas the surface is subject to a net radiative heating of the same amplitude. The change of radiation scheme emphasizes this contrast, which destabilizes the troposphere and provides the fundamental drive for the enhanced tropospheric convection.

3.2. Radiation fluxes

The new radiation scheme corrects the underestimation of the clear-sky OLR at the top of the atmosphere shown by OPE. Higher cloud LWC and the revised longwave optical properties make the clouds radiatively more active in the longwave part of the spectrum. This leads to increased contrast in OLR fields at the top of the atmosphere (Fig. 5b) with marked minima (< 200 W m^{-2}) over convective areas and maxima over clear-sky (> 300 W m^{-2}) or low-cloud-topped areas in agreement with satellite observations. This is an important improvement to the operational scheme (Fig. 5a) which fails to reproduce these features (OLR is in the 230-285 W m^{-2} range in the tropics). The satellite-derived OLR used as reference (Fig. 5c gives the 30-day mean OLR derived by NOAA Climatic Analysis Center from the operational meteorological satellites) is computed from AVHRR measurements on board operational meteorological satellites through a regression between window radiance measurements and total longwave fluxes. When compared to ERBE data, they tend to show smoothed out features with underestimated high values and overestimated low values, therefore, the NEW model OLR, which displays larger contrast, may even be closer to reality than shown in Fig. 5.

The shortwave radiation at the top of the atmosphere is not as drastically modified as the longwave. The operational radiation scheme gives reasonable contrast between high albedo over cloud areas and low albedo over clear-sky oceans when compared to satellite observations. However, this has been obtained for clouds with relatively small liquid water path (LWP) as discussed in Morcrette (1990), a result linked to the highly reflecting model cloud embedded in the operational scheme and to the small value of the proportionality factor relating the saturation water mixing ratio to the diagnosed cloud liquid water content. The new radiation scheme with its new cloud optical properties and higher LWP gives similar global and zonal means

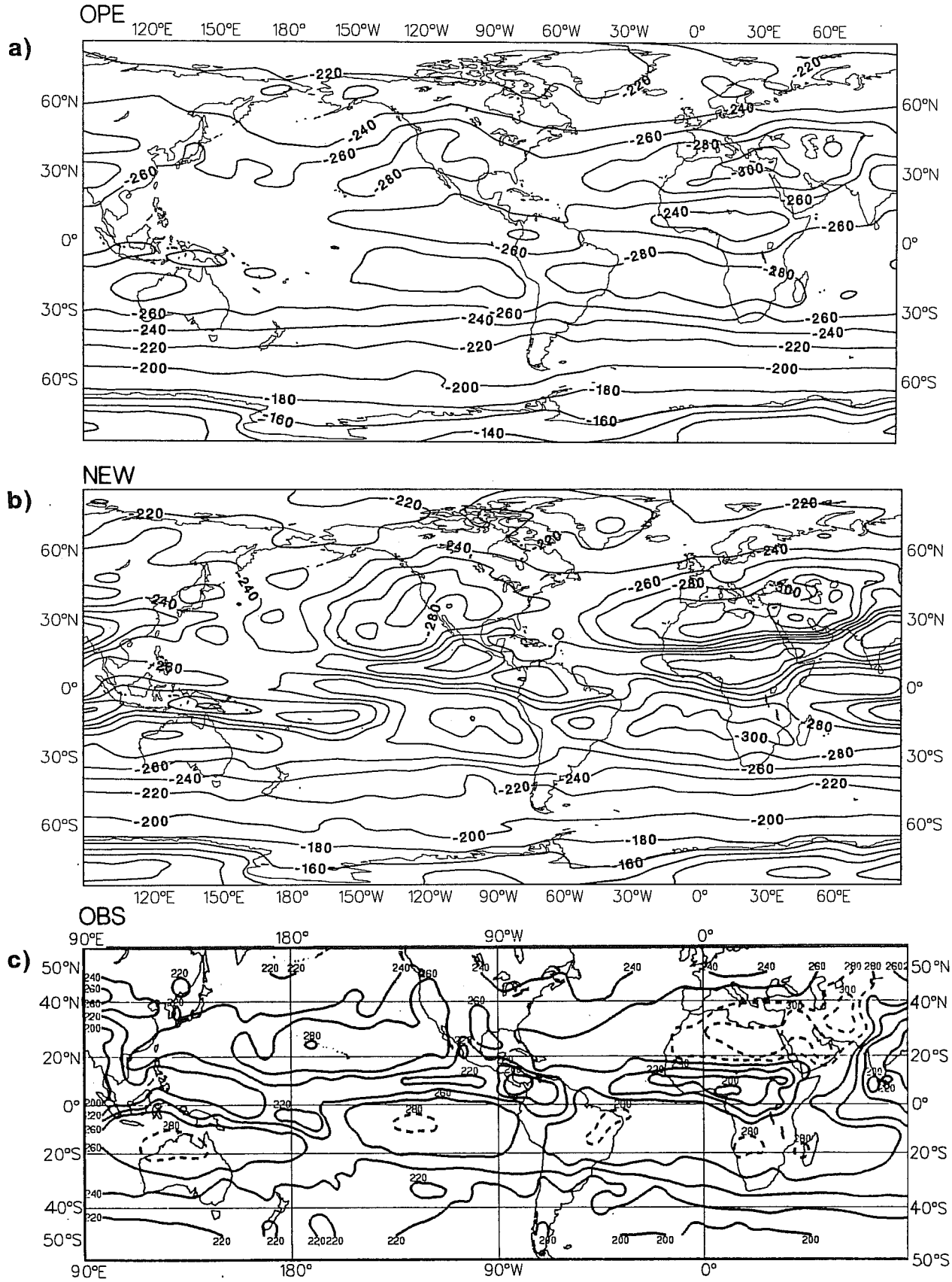

Fig. 5 Outgoing longwave radiation at the top of the atmosphere averaged over the last 30 days of T42 90-day integrations with OPE (top) and NEW (middle). Initial date is 01.06.87,12Z. Bottom figure is the 30-day mean OLR operationally derived by NOAA from AVHRR measurements (NOAA, 1988).

of the shortwave radiation at the top of the atmosphere, but somewhat enhances the longitudinal contrast between clear-sky and cloudy areas.

The direct impact of the revised shortwave H_2O absorptivity is to decrease the clear-sky shortwave atmospheric heating. Therefore, more solar radiation is available at the surface as seen in Figure 6. The increased cloud LWP and modified optical properties contribute to increase the shading effect of the clouds thus increasing the contrast in downward shortwave radiation between clear-sky and cloudy areas (about 40 W m^{-2} less under convective clouds over India and Central America, but about 60 W m^{-2} more in clear-sky areas in the Indian ocean, or West of California and Mauritania).

In the longwave, the new radiation scheme gives larger downward radiation, as a consequence of the better representation of the temperature and pressure dependence of the absorption. In the tropics, this increase is reinforced by the presence of the e-type component of the water vapor continuum. The downward longwave flux also increases in the regions of convective cloudiness. Here again, it leads to more contrast between clear-sky and cloudy areas. These changes in net longwave and shortwave radiation combine and sometimes partially compensate. However, NEW gives larger net radiative fluxes at the surface. North of $60^{o}S$, differences between NEW and OPE are in the range 20 to 60 W m^{-2}.

3.3. Cloudiness

In the ECMWF model, the cloudiness is diagnosed following Slingo (1987). The new radiation scheme uses similar cloud fractions but uses for the "stratiform clouds" the vertically integrated LWP over all clouds diagnosed within the atmospheric slice where either low, medium or high clouds are diagnosed. This makes the formulation of the cloud LWP independent of the model vertical grid structure and usually gives "stratiform clouds" larger LWP than the operational formulation does.

The introduction of the new radiation scheme has an impact on both the vertical and horizontal distributions of the cloud cover. The main features are the increases in convective and high-level cloudiness. For both seasons, the convective cloudiness increases by about 20 and 10 percent over land and ocean, respectively. The high-level cloudiness, which is partly linked to the convective activity in the ECMWF model through the diagnosed anvil cirrus clouds (Slingo, 1987), follows this increase in the tropics. Global means of high-level cloudiness increase between 7 and 11 percent depending

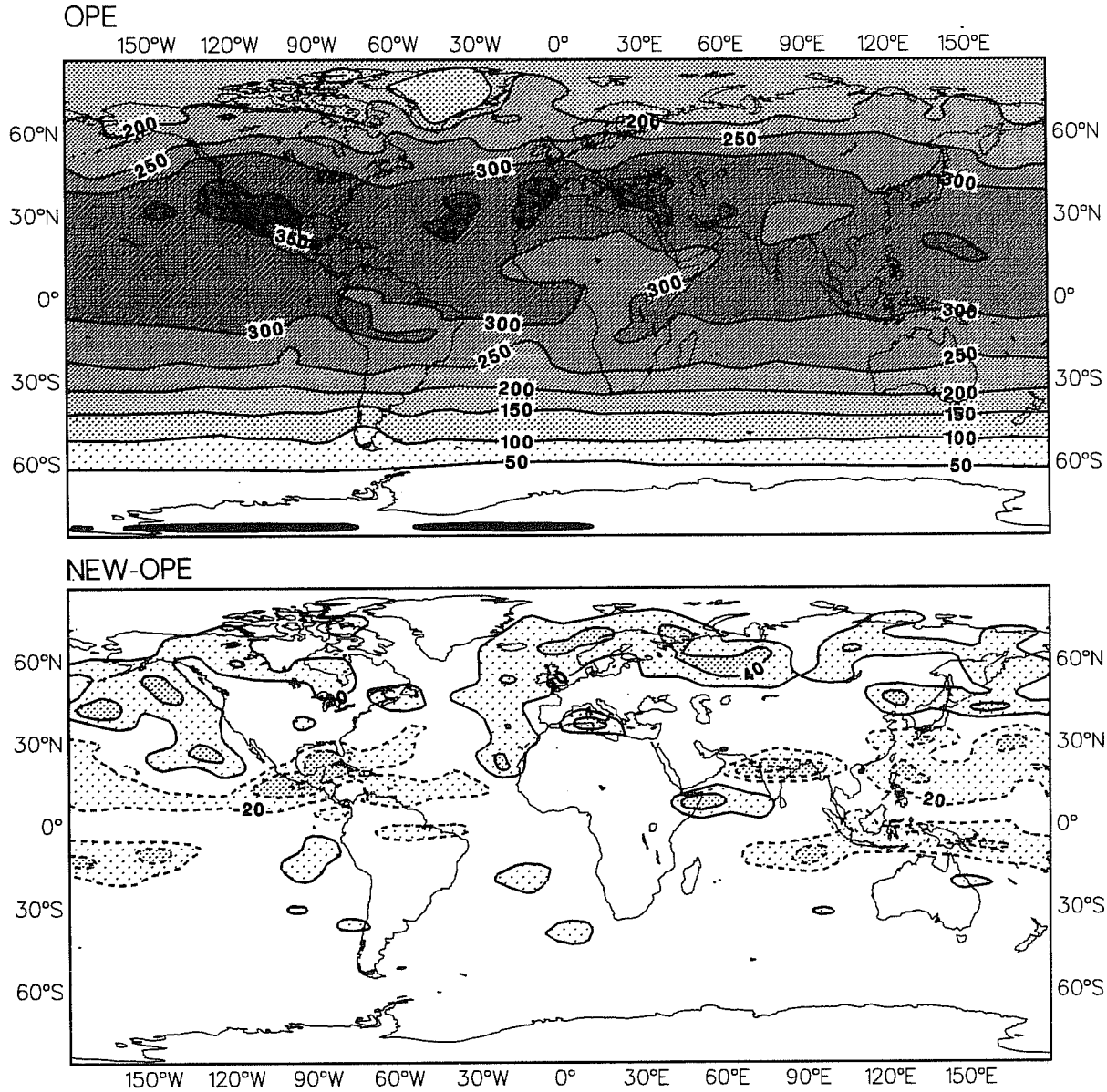

Fig. 6 Net solar radiation at the top of the atmosphere averaged over the last 30 days of T42 90-day integrations with OPE (top: interval is 50 W m^{-2}) and difference NEW-OPE (bottom: interval is 10 W m^{-2}). Initial date is 01.06.87,12Z.

on season and location. The medium-level cloudiness slightly increases in the winter, but decreases in the summer. The low-level cloudiness decrease over land but increases over the ocean.

These changes in the cloud cover are also partly responsible for the differences seen in the radiation fields. However, the main effect, namely the increased contrast between clear-sky and cloudy areas mainly stems from a better description of the radiation transfer in clear-sky conditions and from changes in the cloud optical properties in the radiation scheme.

Experiments by Ramanathan et al. (1983) and Slingo and Slingo (1988) have shown that cloud-radiative effects have the potential to significantly influence the tropical thermal structure, the mid-latitude westerlies, and regional phenomena such as the monsoon. In particular, Ramanathan et al. (1983) have compared the circulations produced by the same model including either optically thick (black) or transparent cirrus clouds. The black clouds provided a strong meridional gradient in the upper level radiative heating, from a strong local as well as a column heating in the tropics to a strong local cooling at polar latitudes. Thus an enhancement of the zonal winds resulted from the intensified equator-pole temperature gradients.

Our results do not show such an effect although the new scheme makes the high clouds much more opaque in the longwave. Most of the experiments with the new radiation scheme display an increase of the zonal mean temperature error by 1 to 2 K over a wide fraction of the atmosphere. This shift in the mean temperature is not accompanied by any significant change in the meridional temperature gradient. In the tropics, the more radiatively active high-level cloudiness with the new scheme is a local heat source which contributes to a destabilization of the upper troposphere and thus leads to rising motion and upper-level mass divergence. However, this enhanced tropical diabatic heating is compensated by stronger eddy meridional transport which explains the small impact on the meridional temperature gradient and the mean zonal winds.

In our integrations with the new radiation scheme, the cloudiness remains relatively stable with respect to its distribution in the control integrations. The total cloud cover generally increases by 2-3 percent in the long T42 90-day integrations with a slight upward shift towards higher-level clouds in the tropics, but no drastic change in the vertical or geographical distribution in the extratropics. Even smaller variations are seen in the T63 and T106 10-day forecasts. Thus the change seen in the height anomaly correlation can chiefly be connected to the effect of the new

radiation scheme and cloud optical properties. The impact on any individual forecast (either beneficial or detrimental) is generally large, usually larger than the impact found by Slingo (1987) of a change of cloud prediction scheme. We can therefore somewhat revise her conclusion "that, for a forecast model, cloud prediction can be at least as important as the parametrization of the radiation transfer". At the time of her experiments, the ECMWF model may have shown a larger sensitivity to cloud distribution than to radiation transfer just because the radiation experimentation (done in relation with the implementation of the 1984 version of the ECMWF radiation scheme (OPE)) was carried out with a cloud scheme (Geleyn et al., 1982) which was giving little geographical and vertical contrast in the cloudiness distribution, and because the cloud experimentation (done in relation with the operational implementation of the 1985 version of the ECMWF cloud scheme) was performed using a radiation scheme (Ritter, 1984) which strongly underestimated the differential radiative heating due to the presence of clouds.

3.4. Diabatic heating rates.

Apart from radiation, the largest responses to a change of radiation scheme are found for the heating by deep convection and vertical diffusion. Impact on the representation of the gravity waves is minimal whereas the heating by large-scale condensation is slightly enhanced in the storm track regions of the extratropics. The increase of the sensible heat flux, specially over the continents is reflected into an increase of the heating of the planetary boundary layer by vertical diffusion. Figures 7 present the zonal mean values of the net radiative heating and of the heating by cumulus convection.

The new radiation scheme increases the net radiative cooling in the subtropics, between 700 and 400 hPa, poleward of 30^{o}N and 10^{o}S in the presented Northern hemisphere summer integration. Effect of the cooling by the e-type component of the water vapor continuum can also be seen with NEW in the lowest layers in the tropics. The heating effect of the high and convective cloudiness is clearly seen in the 10^{o}N region with cooling of less than 0.8 K day^{-1} in NEW and larger than 1.1 K day^{-1} in OPE. In the stratosphere, OPE maintains a +0.50 K day^{-1} warming even after more than 60 days of integration, whereas NEW is closer to radiative equilibrium. In that respect, one of the clearest effects of the new radiation scheme is the

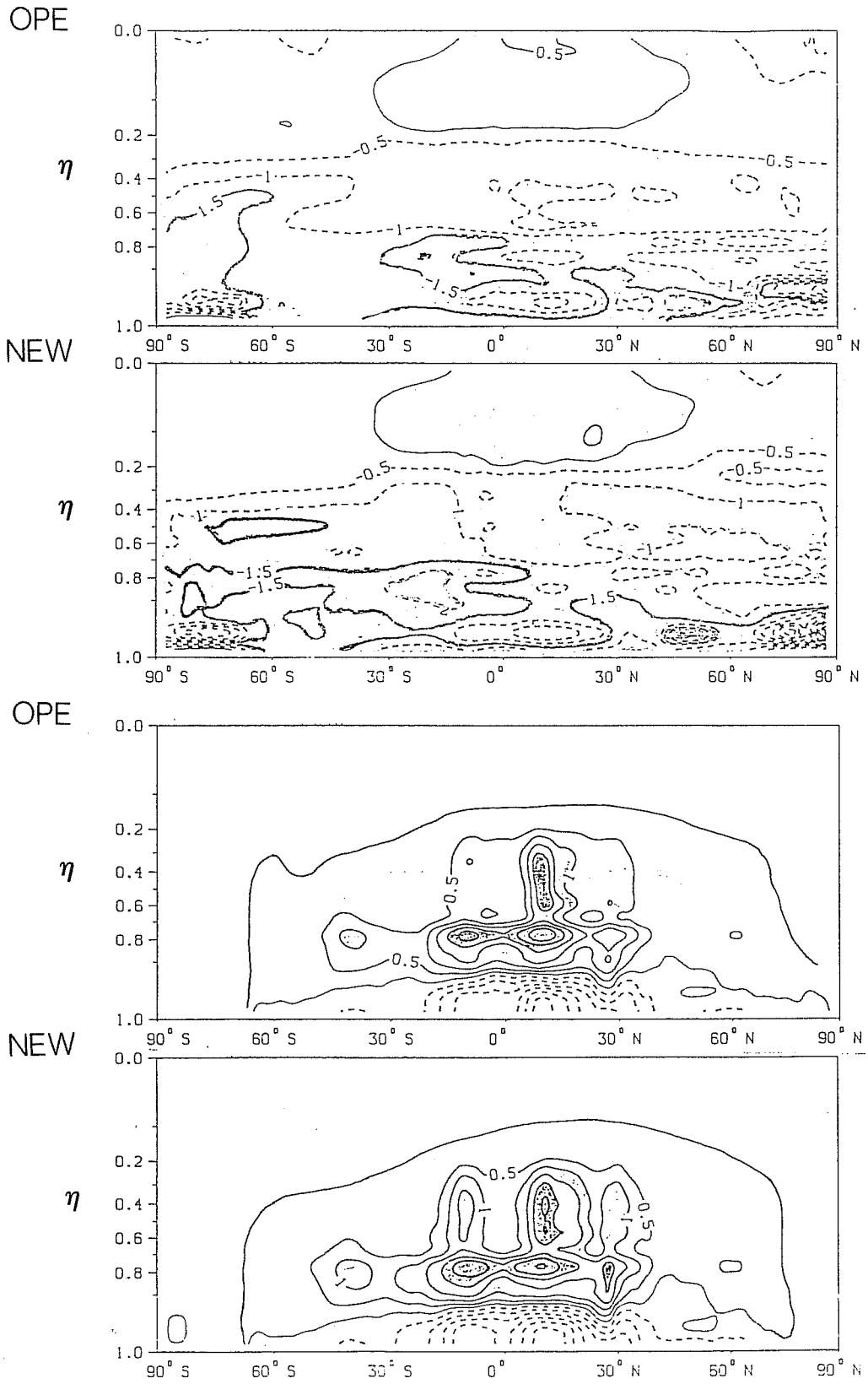

Fig. 7 Contribution of radiation and cumulus convection to the total diabatic heating. From top to bottom, OPE radiative heating, NEW radiative heating, OPE heating by cumulus convection, and NEW heating by cumulus convection. All quantities are in K/day, and correspond to a 30-day average between days 61 and 90 of integrations starting 01.06.87,12Z. Positive quantities between full lines, negative quantities between dash lines.

removal of most of the warm temperature bias in the stratosphere. The globally averaged temperature at 30 hPa changes from 233 to 224 K, that at 10 hPa from 245 to 228 K.

The convective activity is clearly enhanced with NEW, with somewhat larger relative cooling of the lower layers and larger heating of the intertropical region. In this NEW simulation, the secondary maxima in convective heating at 28 ^{o}N and 10^{o}S correspond to more vigourous convection over the Indian monsoon and central Indian Ocean areas as seen in the total precipitation maps. The maxima in convective precipitation over Bengladesh, Sierra Leone, New Guinea, and over the Indian ocean are usually doubled by NEW relative to OPE. This increased convective activity also transports more moisture to the higher tropical layers, where areas of relative humidity higher than 80 percent above 300 hPa are more developed with NEW. This increased relative humidity allows for more high-level cloudiness which, through longwave radiative cooling at the top and relative heating at the bottom, contributes to further destabilization of the upper tropospheric tropical layers.

The new radiation scheme increases by about 2 K the cold bias in tropospheric temperatures (of about 1 to 2 K) displayed by the ECMWF model in T42 90-day integrations. It is important to note that the zonal mean pattern of the temperature error is largely maintained in NEW, so that the impact on the zonal wind error is very small. The relative cooling of the stratospheric somewhat improves the error in zonal wind, but the well documented too strong easterly winds in the high tropical layers appear almost insensitive to the change of radiation scheme.

Our results in the tropics can be simply explained following the approach presented by Betts and Ridgway (1988) after arguments first proposed by Riehl and co-workers (1958, 1979). We consider an idealized energy balance model of the steady-state tropical circulation over the uniform ocean surface that links the tropospheric net radiative cooling, the surface fluxes and the mean subsidence in the descending branch of the Hadley circulation (the regions of deep precipitating convection occupy only a small fraction of the tropics). In this simplified description which neglects horizontal advection and the atmospheric export of heat to higher latitudes, the surface evaporation is coupled to the ascending mass flux in the ITCZ and the compensating subsidence in the descending branch where the surface fluxes compensate the integrated radiative cooling. In this framework, the increased radiative cooling given by the new radiation scheme

is compensated by an increase in evaporation; this extra humidity is transported in the PBL into the ITCZ where it feeds an enhanced convection. The air ascends to exit near the tropopause and gives more convective precipitation. The outflow then descends as a result of radiative cooling, with enhanced subsidence. This quite simple representation is consistent with the results obtained which show larger latent fluxes over the oceanic subtropics, increase in heating by cumulus convection and in convective precipitation in the ITCZ and a stronger Hadley circulation (see error in vertical velocity in Figs.8).

On a global average basis, the changes in mean radiative heating are largely compensated for by changes in the mean convective profiles. Although through opposite experiments (their initial modification of the convective heating profiles was compensated for by changes in radiative heating), these results corroborate the findings of Albrecht et al. (1986) that the problems of the parametrization of cumulus convection and of cloud-radiation interactions are intricately coupled.

3.5. Eddy activity

As discussed by Arpe (1988), one of the systematic errors of the ECMWF model is the drop of eddy energy (eddy available AE and eddy kinetic KE) and increase of zonal energy (zonal available AZ and zonal kinetic KZ) during the course of the forecasts. According to Arpe (1988), this feature is mainly related to the reduction of the transient waves as the standing waves contribute little to the total eddy energy.

Together with latent heat release and sensible heat transfer, radiation produces differential heating and thus generates available potential energy. Compared to the operational scheme, the new radiation scheme increases the contrast between the tropics, where local relative radiative heating is now found under the more radiatively active high-level cloudiness, and the subtropics where a larger clear-sky radiative cooling prevails. This effect is further enhanced by the increase in latent heat release in the tropics. As seen in Table 4, the effect of the more realistic net radiative cooling of the new radiation scheme is to give the model an enhanced energy cycle, at all wavenumbers, from the forecast start as well as after a long range integration. In that respect, the new radiation corrects at least partly the problem mentioned above. A higher level of eddy activity is obtained through

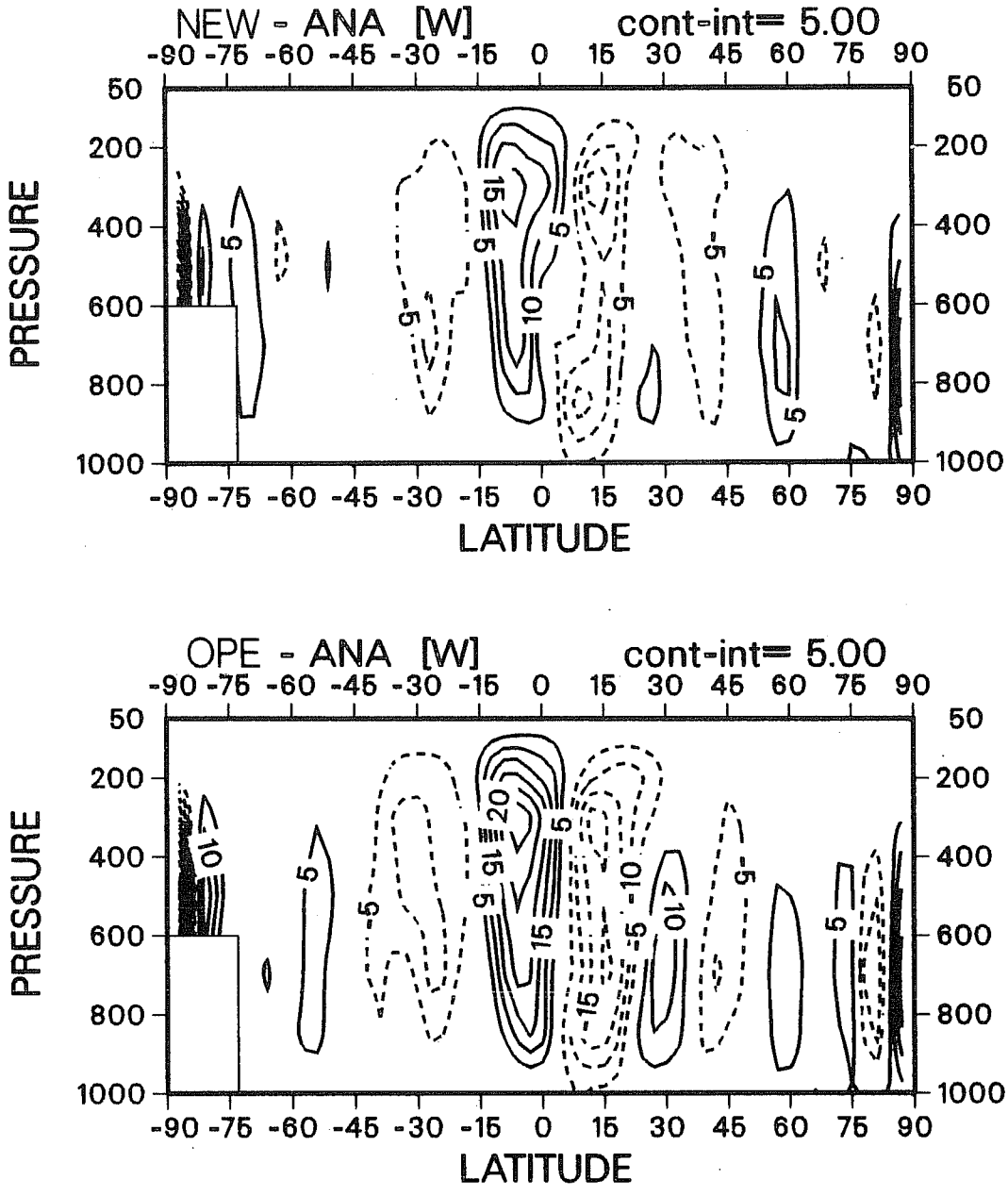

Fig. 8 Zonal mean error in vertical velocity (10^{-3} Pa s^{-1}) averaged over days 61 to 90 of T42 summer simulations with OPE (bottom) and NEW (top). Initial date is 01.06.87, 12Z.

Table 4: Box diagram of the energy cycle of fht model averaged over the last 30 days of T42 90-day integrations with OPE and NEW. First panel is the corresponding analyzed values. Initial data is 1.12.87,12Z. Energy terms are in kJ m^{-2}, conversion terms in W m^{-2}.

ANALYSIS

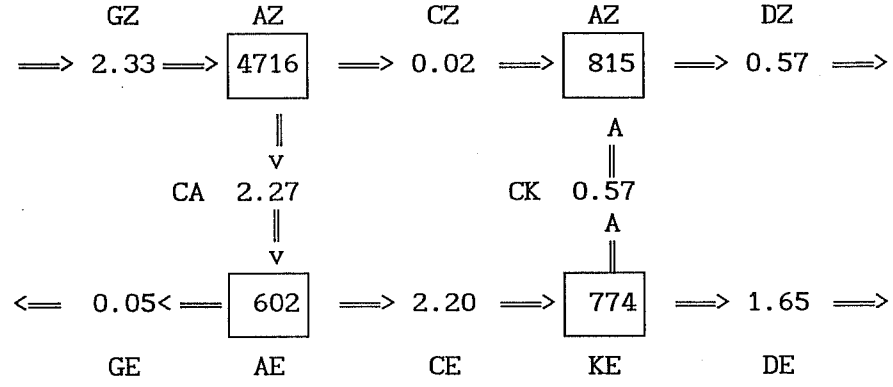

OPE

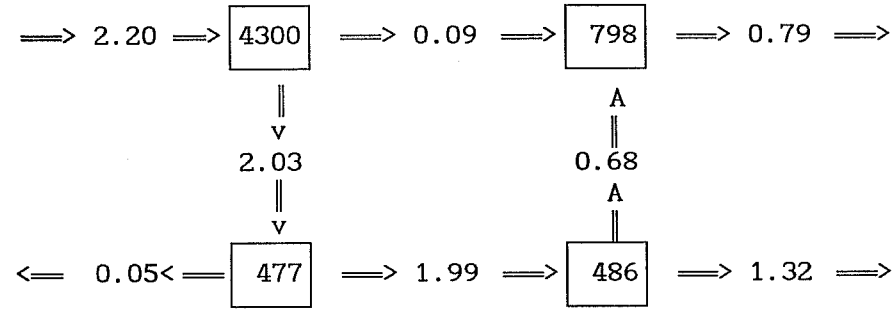

NEW

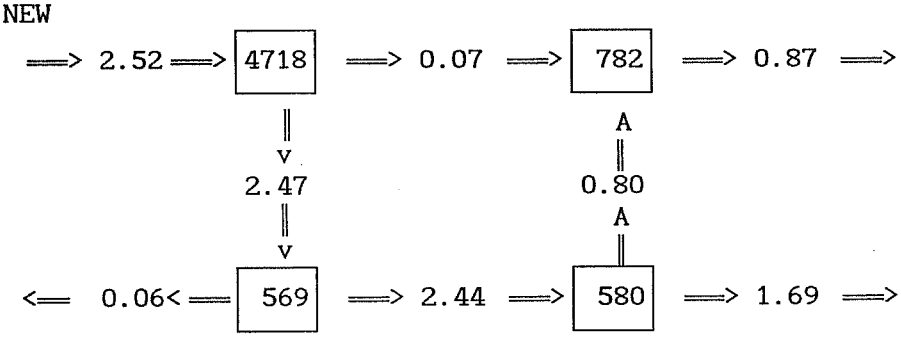

(i) an increase in GZ, the generation of AZ, (ii) a higher AZ (now in good agreement with its analysed value), (iii) an increase in CA, the conversion between AZ and AE, (iv) a higher AE (in better agreement with its analysed value), (v) an increase in CE, the conversion between AE and KE. The

improvements are clear in terms of both the latitudinal distribution of AE and KE and of their temporal evolution.

Results of the experimentation discussed above also show that the new radiation scheme contributes to a partial correction of some errors of the ECMWF model. The weakening of the trade winds and the weakening of the transients in both tropical and extratropical latitudes are much reduced. The new scheme also increases the low frequency variability (above 5 days) of the model. As far as a cloud-radiation interaction mechanism is concerned (Ramanathan, 1986), the new scheme should also make the model more sensitive to tropical SST anomalies.

4. RADIATION AS A DIAGNOSTIC TOOL FOR MODEL VERIFICATION

The new radiation scheme gives clear-sky radiation fields at TOA in much better agreement with satellite-derived radiation fields. Then any comparison of model-generated and satellite observed radiation fields over cloudy areas will allow to address more specifically questions related to the model representation of the cloudiness.

Whatever the uncertainties in an observed cloud climatology, the observed diurnal and seasonal variability of cloudiness are very strong signals which stand out above these uncertainties, and any cloud forecasting model, to be said successful, should be able to reproduce these signals with good fidelity. Although the seasonal cycle is certainly a very important signal to reproduce, the validation of the diurnal cycle is more directly relevant and easier to be carried out for a medium-range forecast model, such as the ECMWF operational model. The direct observed coupling between convective activity and cloudiness is needed to properly simulate the role of cloudiness in regulating the hydrological cycle.

Comparisons between satellite-observed and model-generated diurnal cycles of outgoing longwave radiation have been hindered by numerous obstacles. A meaningful comparison requires consistence in the space and time sampling of the compared fields as well as in their geometrical and radiometric characteristics. Up to now, similar comparisons of model outputs with observations (on a time average basis, usually) have used satellite measurements modified as to obtain a quantity comparable to the model-generated quantity ("satellite-to-model approach"). That process usually introduces at best some uncertainties, at worst some inconsistencies. These may be linked either to an insufficient sampling of

the diurnal cycle (as with measurements from an unique polar-orbiting satellite), to the satellite viewing geometry and the subsequent necessity to account for limb darkening in the measurements, or to the narrow-band channel satellite measurement and its conversion to a broad band data.

Similarly, the validation of the cloudiness forecast by a large-scale atmospheric model through comparisons with observations is a difficult exercise due to problems inherent to the retrieval of an "observed" cloudiness from satellite observations of radiances (Slingo, 1987). If model cloudiness, either diagnosed or prognosed via a cloud generation scheme is clearly defined in all its characteristics, observed cloud parameters such as fractional cover, top temperature and emissivity are highly dependent on the type of observations (spatial and spectral resolution of the radiometer, time and space sampling of the data) and on the retrieval algorithm (definition of the background clear-sky radiance and of the threshold values for threshold-type methods, definition of the learning set for statistical methods, role of the radiation scheme and of the optical characteristics assumed for the model clouds in the methods based on a radiative transfer analysis) (see Rossow et al. (1985) for a detailed discussion of the methods and problems related to the extraction of the cloud cover from satellite-observed radiance measurements).

This section presents results of an attempt at limiting those uncertainties and inconsistencies in the comparison of satellite observations with model outputs by taking an opposite approach ("model-to-satellite approach") the interest of which was illustrated by Morcrette (1988). We have modified some outputs of the diagnostic package of the ECMWF forecast model to simulate as closely as possible measurements of the brightness temperature (T_B) in the longwave window channel of METEOSAT, from the temperature, humidity, and cloudiness profiles operationally produced by the model. A more complete description of the methodology can be found in Morcrette (1989b).

For such a validation of the diurnal cycle, the only satellite data available at present with adequate time sampling come from geostationary satellites. The observational data used in this study are METEOSAT longwave window channel measurements compiled for July 1983 in the so called B3/CX format of the International Satellite Cloud Climatology Project (ISCCP; Schiffer and Rossow,1983, 1985). A full description of the ISCCP reduced resolution global radiance data set is given in WMO-ICSU (1985), with details on the navigation, calibration, and time and space sampling data

processing. From fields of temperature, humidity and cloudiness forecast by the model, the radiance in the longwave window channel of METEOSAT is simulated using a longwave radiation scheme modified to compute channel radiances in the METEOSAT geometry, i.e., using the viewing angles of observation. The radiance is then converted to brightness temperature taking into account the filter function of the METEOSAT longwave window channel as given in WMO-ICSU (1985).

Some limited areas (10.125 x 10.125 deg^2, corresponding to 9 x 9 T106 grid boxes) are then defined, over which we have concentrated our study. These areas are small enough in their extent to encompass a relatively homogeneous background surface and, if possible, weather regime characterized by a unique type of cloudiness. They are large enough to include a statistically significant number of grid boxes. Over these limited areas, the diurnal variations of the cloudiness and related brightness temperature as seen in the METEOSAT measurements and as produced in the model are studied using evolution histograms of the observed and simulated T_B's to assess the quality of the representation of the diurnal variations of the surface-atmosphere system by the ECMWF model.

Duvel and Kandel (1985) have illustrated the potential of the evolution histogram of the brightness temperature (hereafter EH (T_b)) to study the diurnal variations of the surface-atmosphere system from satellite observations. In EH (T_b), the x-axis represents the time evolution whereas the y-axis is the brightness temperature scale. Isolines define fractions of the total number of picture elements within each temperature class (taken as 1 K wide in our study). The warmer T_B then correspond to radiation coming from the surface and the colder to radiation emitted by the clouds.

In Figures 9 to 14, we compare the EH (T_b) for the METEOSAT longwave window channel T_B over some limited areas. The left panels correspond to the ISCCP/B3 observations averaged over the T106 grid and the right panels correspond to the model-generated T_B's corresponding to the EC2 radiation scheme. Main difference in behaviour of observed EH (T_B) between oceanic and continental areas is obviously the weak or non-existing diurnal variation of sea surface temperature (Figs. 9 and 11) compared to the large variations of the surface temperature (5-30 K) appearing in the observed EH (T_B) in the land areas (Figs. 12 and 13).

The three first areas are located over the ocean, with different types of cloudiness resulting from their latitude and prevailing circulation regime. The Cape Verde Island area (Figs. 9) is located within a zone of

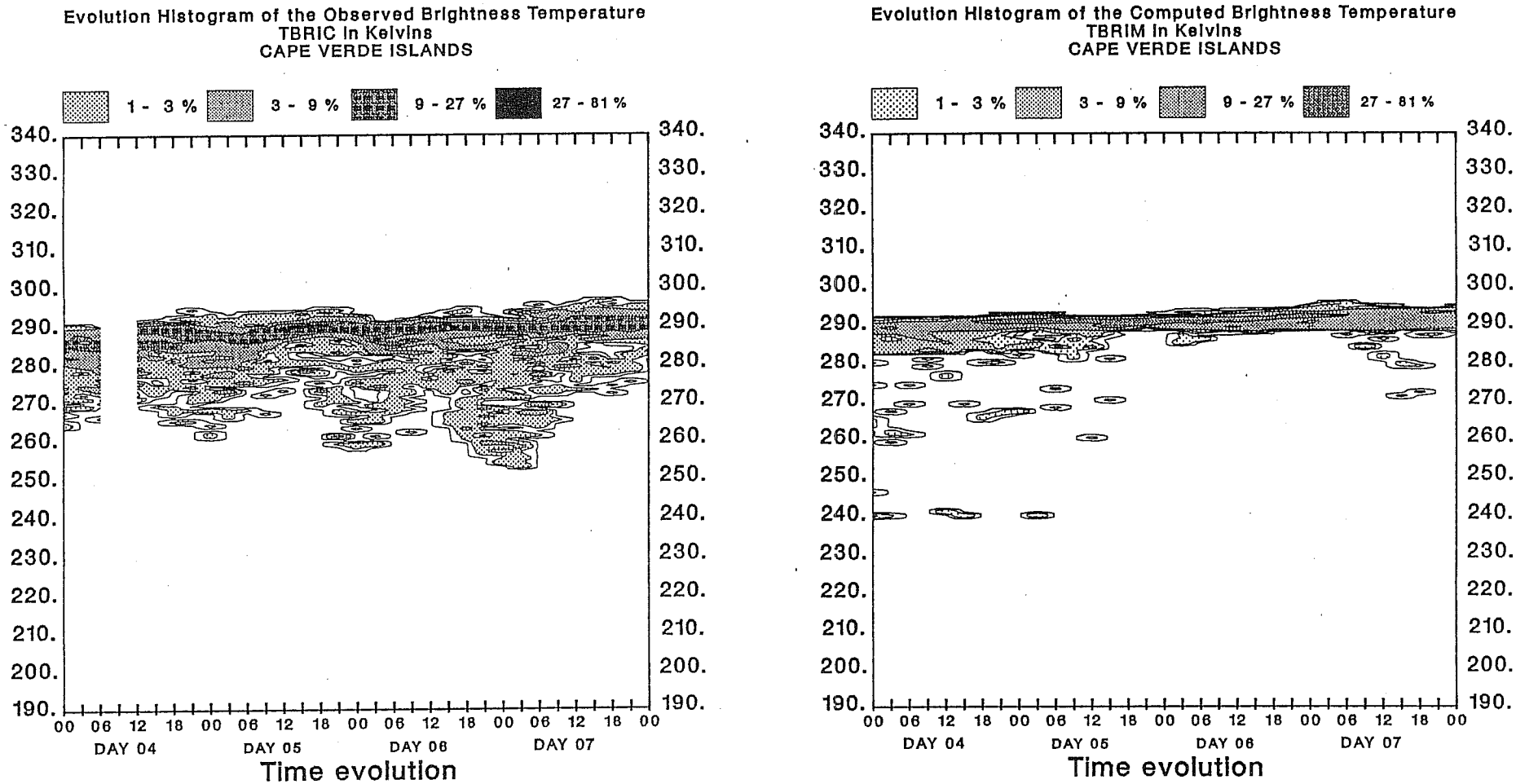

Fig. 9 The evolution histograms of the window brightness temperatures for the Cape verde Island area (26N-16N, 28W-18W). Left panel is the evolution histogram from ISCCP/B3 data averaged over T106 grid boxes; right panel is the evolution histogram produced by window brightness temperatures simulated from T, q, and cloud fields forecast by the ECMWF model including the EC2 radiation scheme.

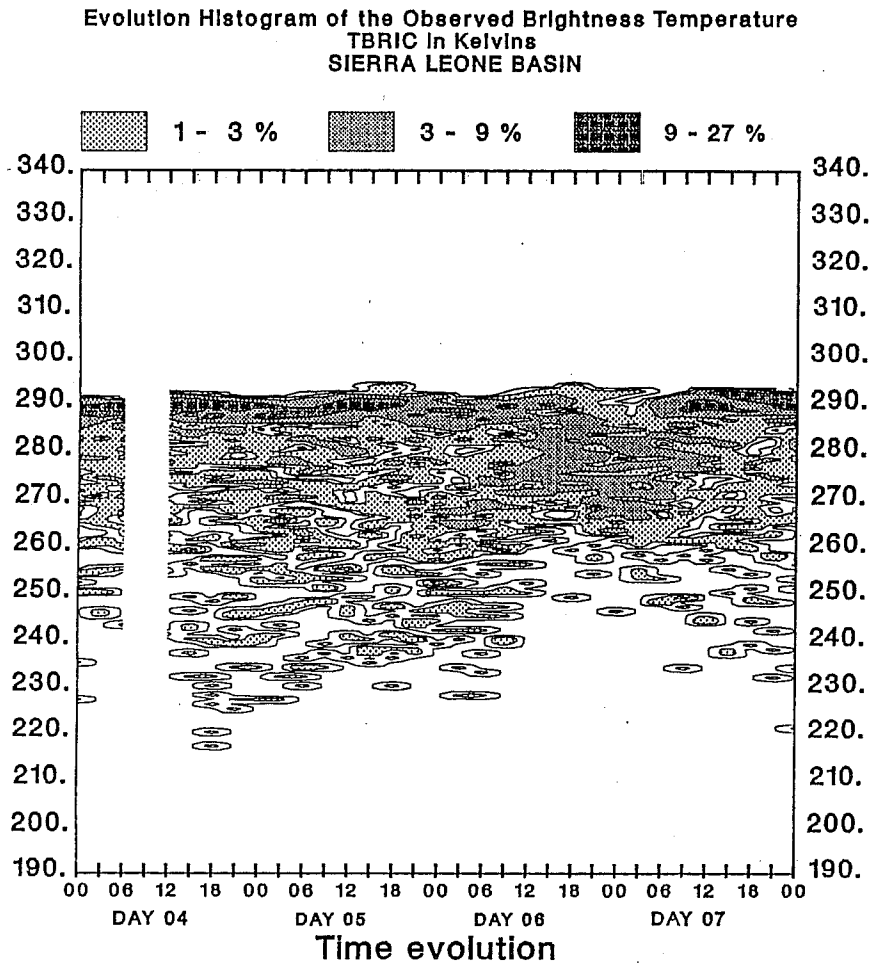

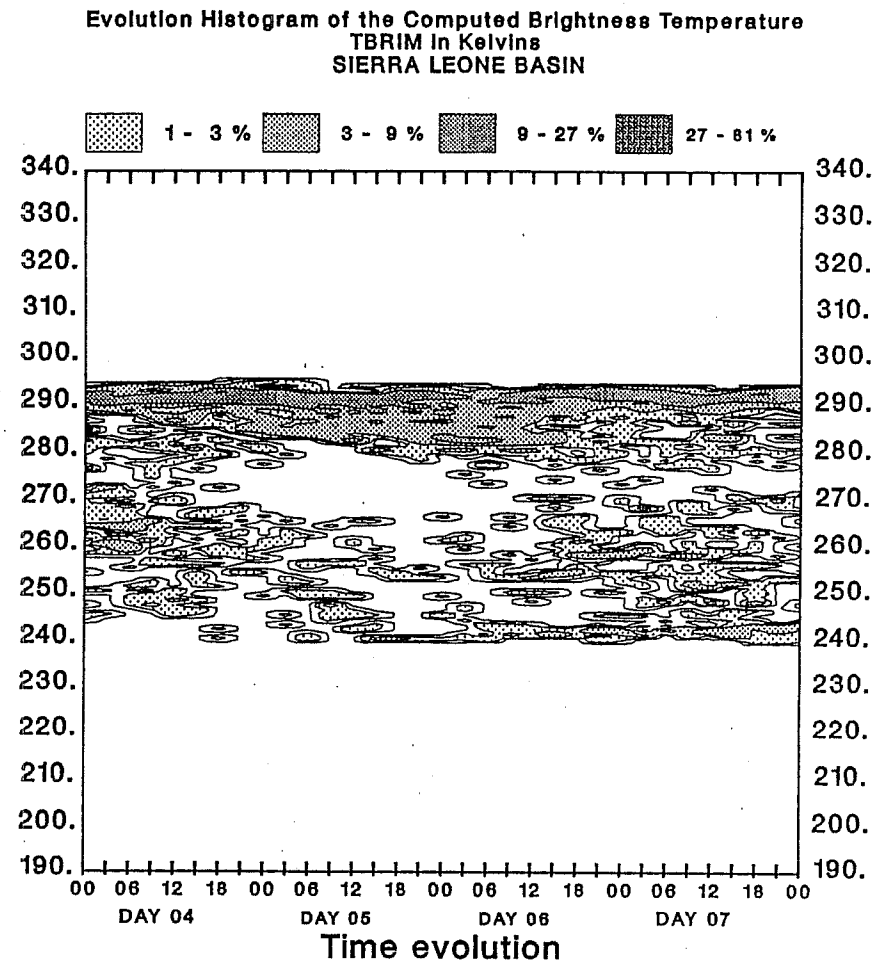

Fig. 10 As in Fig. 9, but for the Sierra Leone Basin area (16N-6N, 34W-24W).

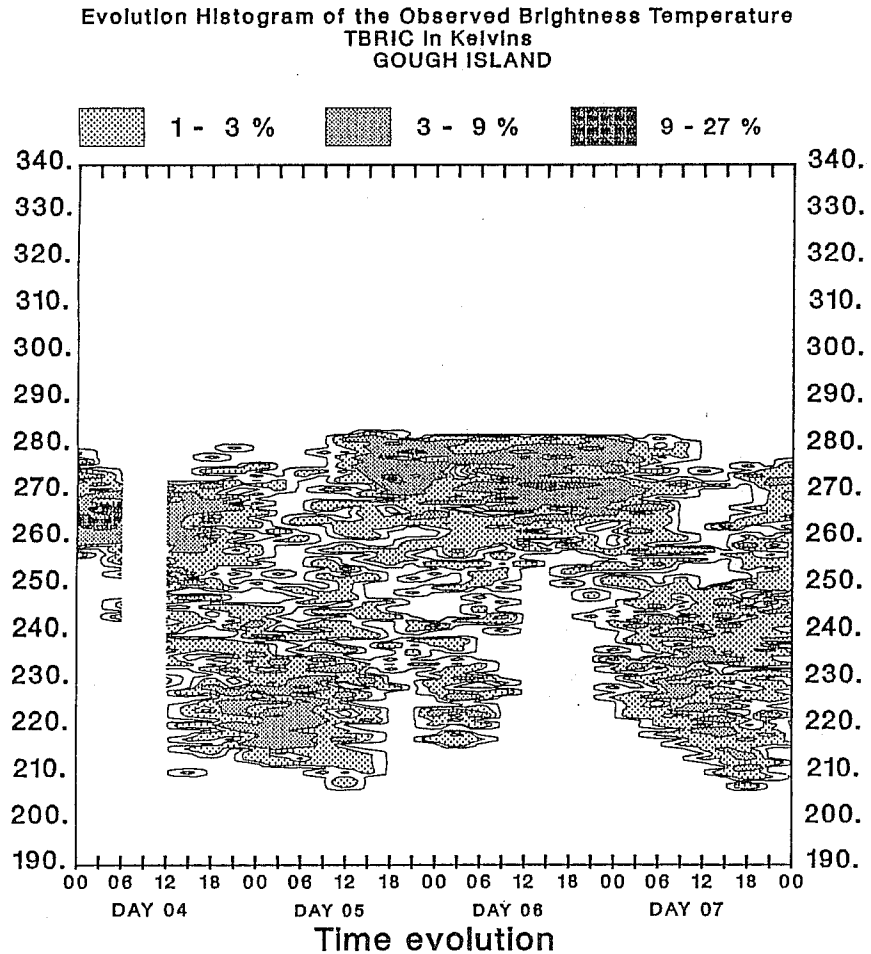

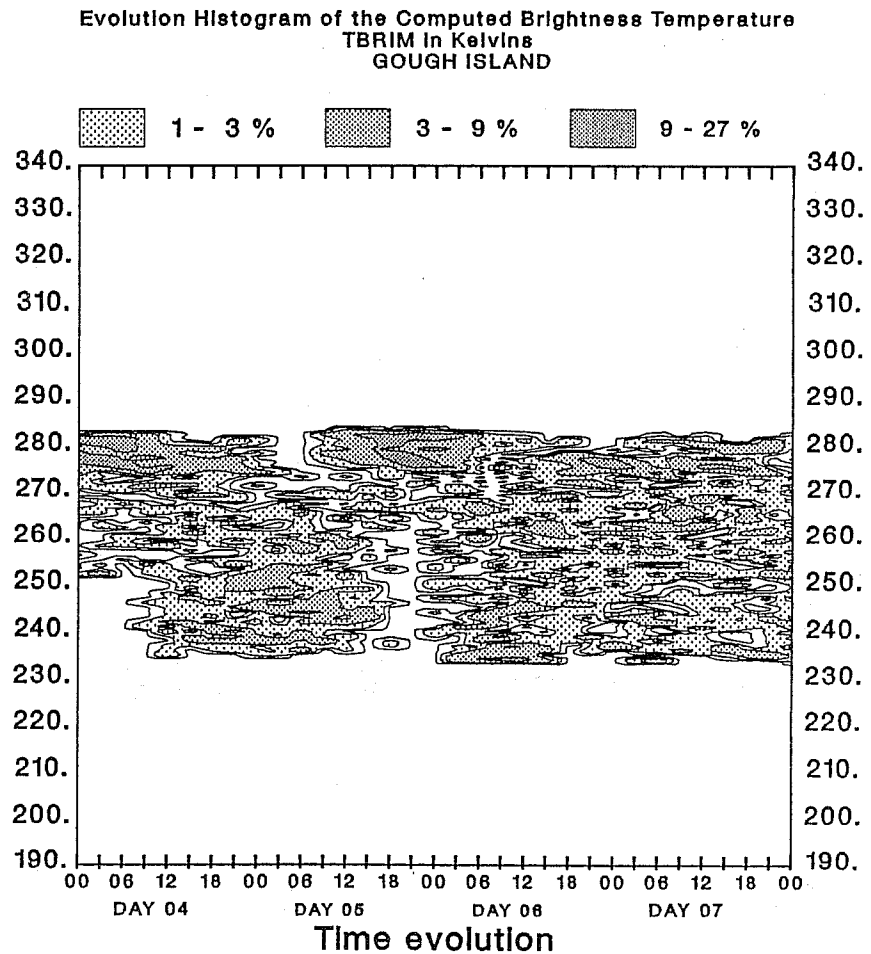

Fig. 11 As in Fig. 9, but for the Gough Island area (39S-49S, 16W-6W).

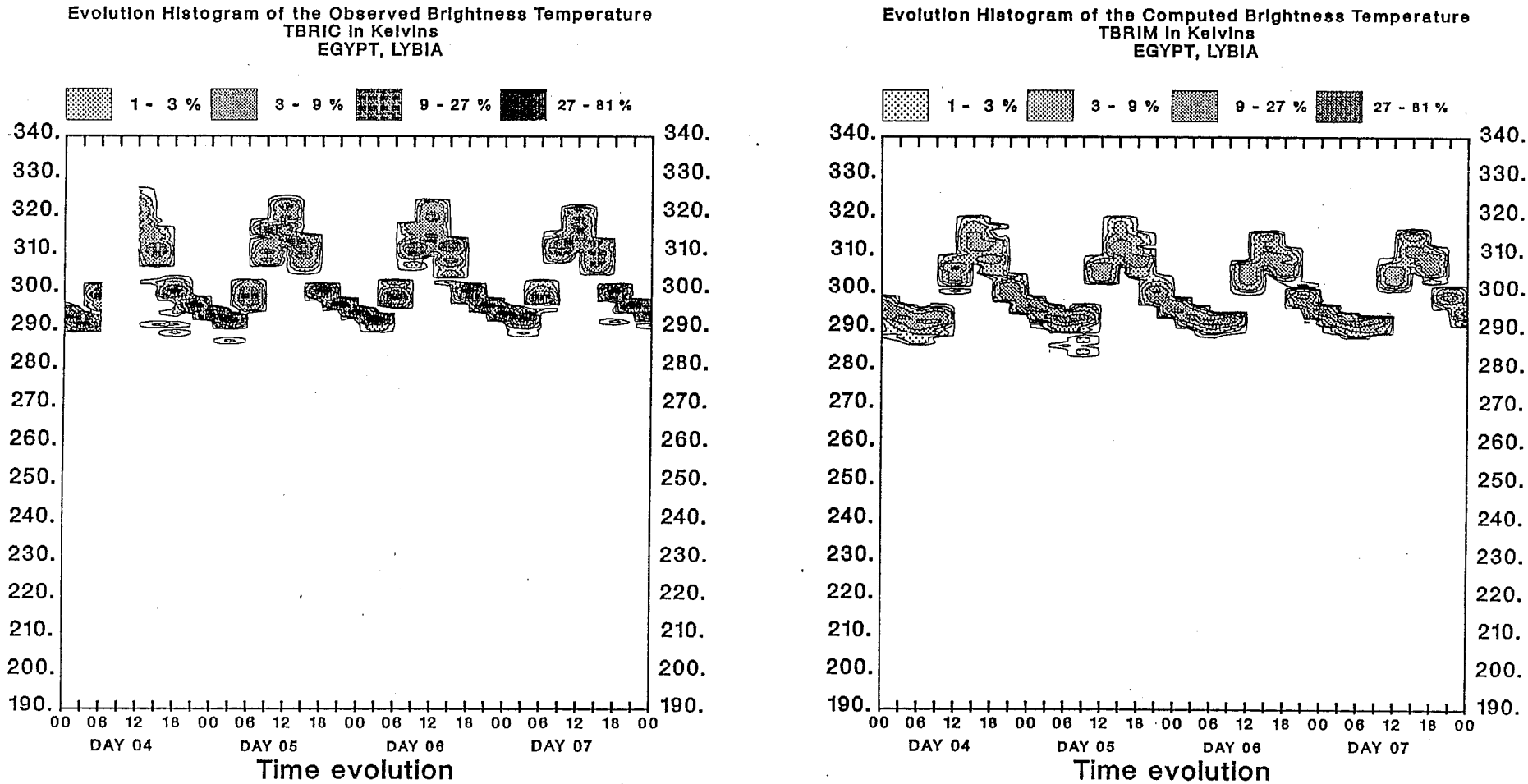

Fig. 12 As in Fig. 9, but for the Egypt-Lybia area (29N-19N, 20E-30E).

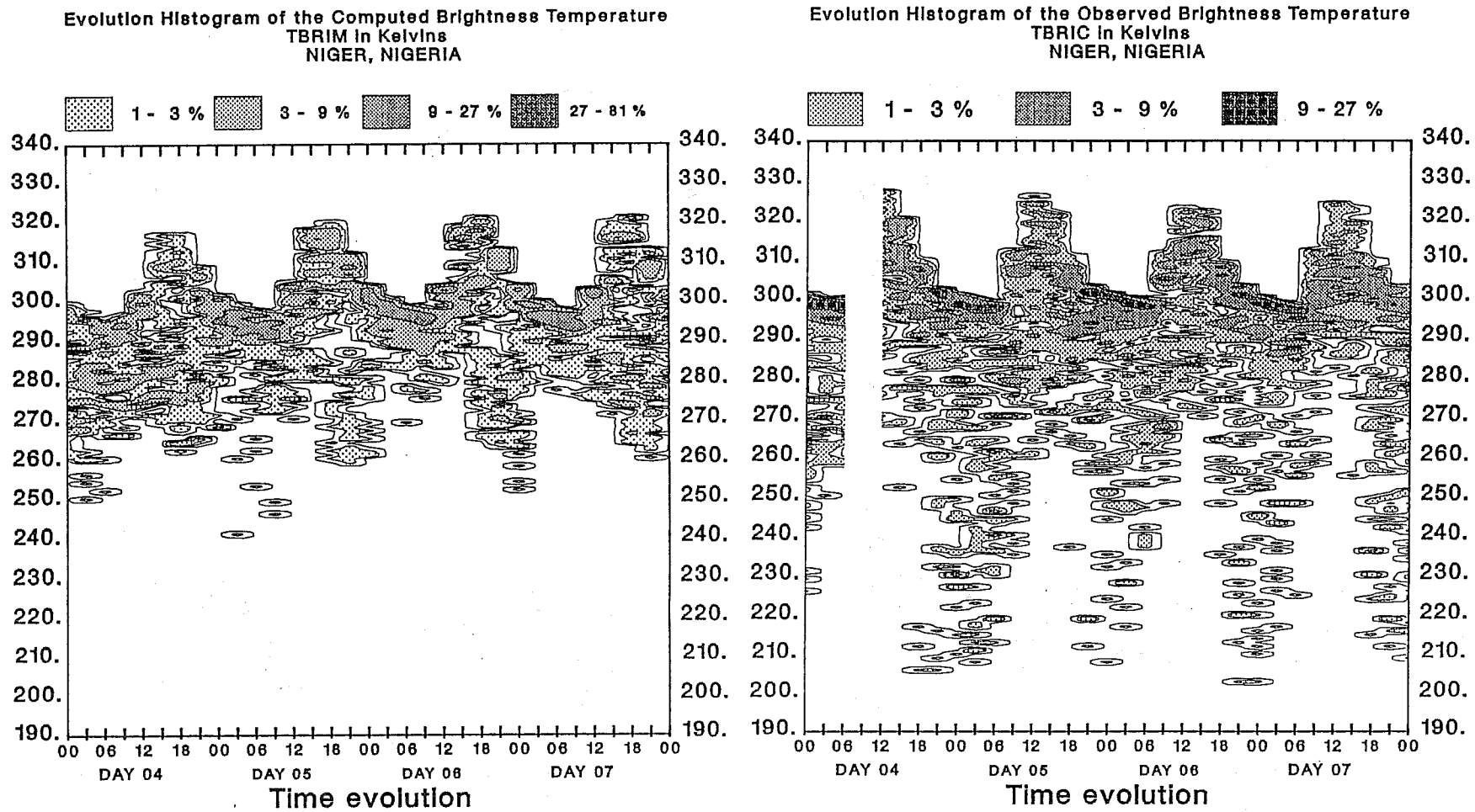

Fig. 13 As in Fig. 9,but for the Niger-Nigeria area (20N-10N, 5W-5E).

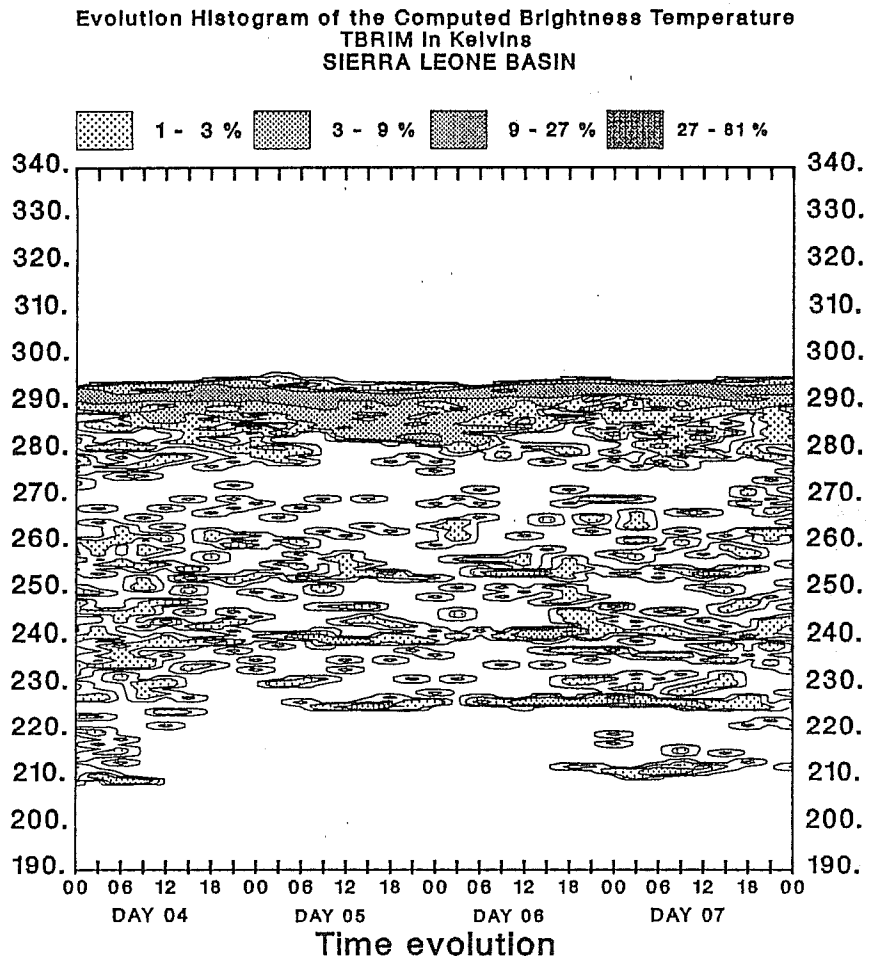

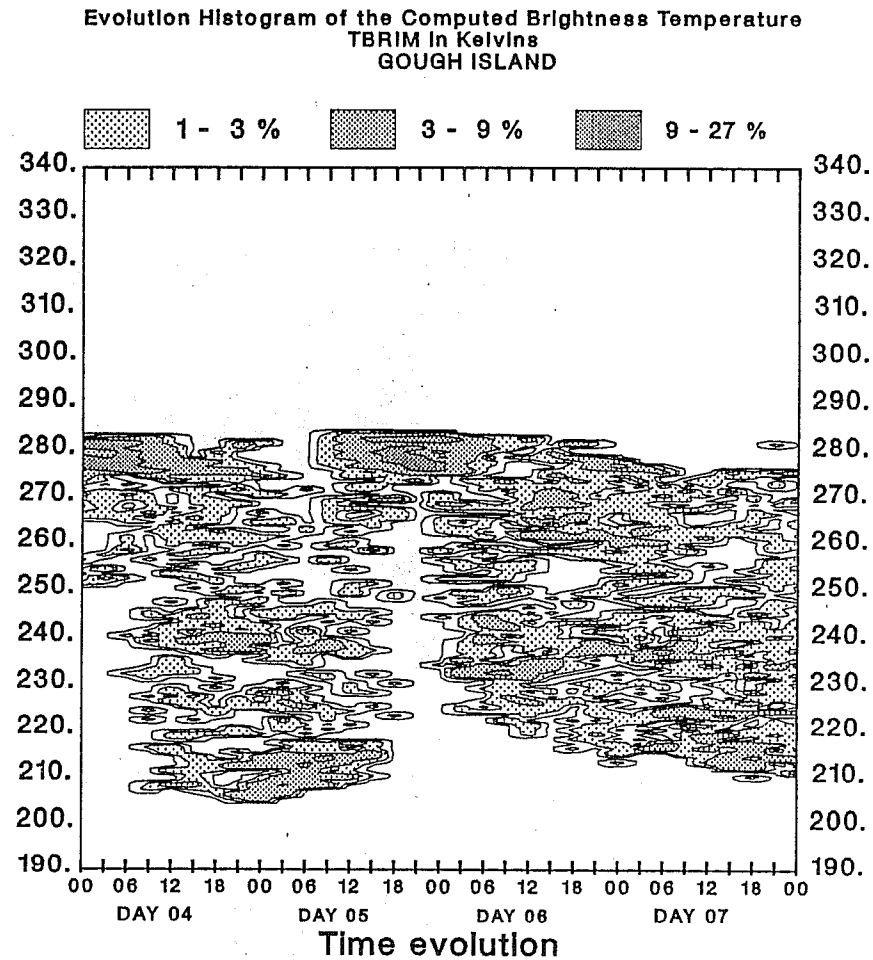

Fig. 14 The evolution histogram produced by window brightness temperatures simulated from T, q, and cloud fields forecast by the ECMWF model including the EC3 radiation scheme over the Sierra Leone Basin (cf. Fig. 9), the Gough Island (cf. Fig. 11) and the Niger-Nigeria (cf. Fig. 13) areas.

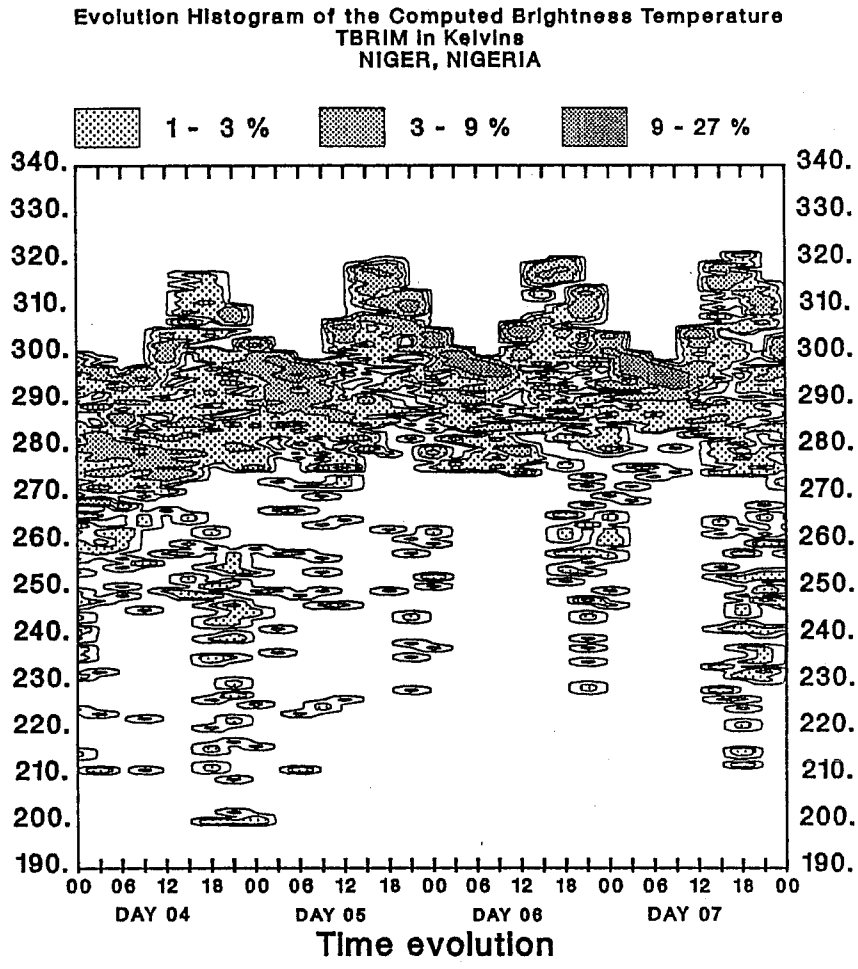
Evolution Histogram of the Computed Brightness Temperature
TBRIM in Kelvins
NIGER, NIGERIA
1 - 3 %
3 - 9 %
9 - 27 %
340.
330.
320.
310.
300.
290.
280.
270.
260.
250.
240.
230.
220.
210.
200.
190.
00 06 12 18 00 06 12 18 00 06 12 18 00 06 12 18 00
DAY 04
DAY 05
DAY 06
DAY 07
Time evolution

Fig. 14c

persistent stratiform clouds formed by subsidence above cold oceanic currents along the subtropical western side of the African continent. The low stratiform clouds display a marked diurnal cycle. The low-level cloud layer is thicker during the night (with a somewhat high top level at cooler temperature giving a smaller T_B). In response to the diurnal cycle of insolation, it becomes thinner and lower during daytime, giving larger T_B. The Sierra Leone Basin area (Figs.10), located in the oceanic ITCZ, displays an observed EH (T_B) characteristic of quasi-permanent convective activity with no marked diurnal cycle. The Gough Island area is located in the storm tracks of the Southern hemisphere. Frontal cloud systems are passing through the area during the period study, giving a mostly cloudy to overcast sky. No particular diurnal cycle can be seen, but the observed EH (T_B) shows a large cover of optically thick high-level clouds.

The areas over land correspond to different types of soil and vegetation. Desert barren soil prevails over Egypt-Lybia (Figs. 12). This area displays a diurnal cycle of the CFD corresponding to mostly clear-sky conditions. Minimum surface T_B is found during the night (00 GMT), and maximum T_B occurs at 12 GMT. Interestingly enough, during daytime, the inhomogeneities in soil properties and thus in surface temperature give a spread of 10 K or more in the observed T_B's. The other land area presents EH (T_B) showing the presence of cloudiness. The Niger-Nigeria area is covered by grassland with sparce shrub. Comparisons of Figs. 12 and 13 show that the denser the vegetation, the smaller the T_B's and the narrower the range of diurnal variation of the warmest T_B's.

Comparison of observed and model-generated EH (T_B) allows to pinpoint various deficiencies in the representation of surface-cloud-radiation interactions in this version of the ECMWF model. For example, in Figs.12, the model diurnal cycle of surface temperature is smaller than the observed one by about 5 K as the maximum model T_B is 320 K compared to the observed 325 K around 15 GMT. In such clear-sky dry conditions, this defect might be related to an inappropriate surface resistance for the transfer of heat. Similar features are seen over the other land area although the model is successful at diminishing the amplitude of the diurnal cycle of the surface temperature when the vegetation cover increases.

As already discussed by Slingo (1987), the cloudiness present over the sub-tropical oceans offers a challenge to the modeller. The extended stratiform clouds of the Eastern façade of the continents are vertically sub-grid scale whereas the trade-wind cumuliform clouds are horizontally

sub-grid scale. As seen in Figs. 9, the present ECMWF model does not produce any reasonable representation of the stratiform clouds.

Where high cloudiness prevails in the observations (Figs. 10, 11, and 13), the longwave radiative impact of the cloudiness is clearly underestimated with the EC2 radiation scheme (right panels). This can be explained by either a too small, a too low or a too transparent cloud cover. The comparison of EH (T_B) over areas in the storm tracks (Figs. 11), where the model is known to be quite successful at diagnosing the frontal clouds from relative humidity (Slingo, 1987), corroborates the findings of section 2, namely the presence of too transparent high clouds. Over land this problem gets worse as convective clouds are assigned too small a maximum cloud fraction (20 percent). Moreover, there is a difference between model and observations in the characteristics of the diurnal cycle over land (Figs. 13). Maximum surface temperature is observed between 12 and 15 GMT, and maximum convection is seen between 21 and 3 GMT. The model represents relatively well the phase, but not the amplitude of the diurnal cycle of the surface temperature; the minimum T_B corresponding to maximum vertical extent of convection usually appears too early in the afernoon around 18-21 GMT. Over the convective oceanic area, the model produces too few medium-level clouds as shown in Figs. 10. In the new radiation scheme (see Figs. 14), better cloud properties, specially for the high-level cloudiness, improve the agreement between model-generated and observed EH (T_b).

5. CONCLUDING REMARKS AND PERSPECTIVES

Among all sub-grid processes whose effects have to be parametrized in a large-scale numerical model of the atmosphere, radiation transfer is a physical process for which there is a relatively firm physical basis and an extended albeit uncomplete set of observations. Radiation fields (but only at the top of the atmosphere, so far) are quantities that can be validated on a global scale with a reasonable temporal and spatial resolution thanks to the satellite measurements. A theoretical description of radiation transfer has been known for decades. Compilations of spectroscopic parameters for the most important radiatively active constituents of the atmosphere are available. Very accurate models such as the line-by-line models can be used to compute reference values of the clear-sky fluxes. In its development, the new radiation scheme has been carefully checked against such accurate models for both the longwave (Scott and Chédin, 1981;

Morcrette and Fouquart, 1985) and shortwave ranges, and validated against satellite measurements.

This paper is an illustration of the worth of the Intercomparison of Radiation Codes in Climate Models (ICRCCM) programme. The availability through that programme of detailed line-by-line and narrow-band model results for a set of standard clear-sky and cloudy atmospheres has made possible to complete a thorough assessment of deficiencies present in earlier versions of the ECMWF radiation scheme and has helped in validating a new scheme. The successive versions of the ECMWF radiation scheme were qualitatively described, and the deficiencies present in the earlier versions of the scheme were documented. The comparisons with detailed model results shed light on the following points:

- the overestimation by EC1-EC2 of the shortwave H_2O absorptivity which leads to too large shortwave atmospheric absorption (by up to 20 percent) and too small downward shortwave radiation at the surface (by 5 to 10 percent);
- the underestimation by EC1 and EC2 of the longwave radiative cooling, with main errors in the lower troposphere with EC1, and between 700 and 300 hPa with EC2. As a consequence, EC1 and to a smaller extent EC2 underestimate the clear-sky outgoing longwave radiation at the top of the atmosphere;
- the exaggerated sensitivity of EC1 to small amounts of scatterer, a problem corrected in EC2;
- the use by EC1 and EC2 of an unrealistic model cloud for computing off-line the cloud radiative parameters which has prevented these schemes from properly representing both the shortwave planetary albedo and OLR for realistic cloud liquid water contents.
- the better performance of EC3, which corrects most of these deficiencies, and gives results in better agreement with those of more detailed models.

This paper also summarizes the results of a study carried out with the ECMWF model in which a large number of integrations have been performed using the EC2 radiation scheme or a revised radiation scheme (EC3). The direct impact of this new scheme can be seen in

(i) more realistic radiative flux divergences, which are underestimated in the operational scheme. As a result, the model becomes more active;

(ii) more correct outgoing longwave radiation at the top of the atmosphere, most noticeable in areas of tropical convection due to a more realistic radiative response to clouds. This feature is in particular important for

verification against satellite observations.

(iii) increased solar radiation at the surface. This is significant for predicting surface temperatures over land and for the thermal forcing by land-sea contrast.

Moreover, the new radiation scheme contributes to partially correct through various interactions a number of systematic errors of the ECMWF model: as such the introduction of this radiation scheme in the ECMWF operational forecast system has an impact on the analyses through the first guess forecast. From the comparisons discussed above, it is likely to affect the divergent flow, but also the surface fields. These changes are of importance for ocean modellers who use those fields as a forcing for their models.

The new radiation scheme, which has become the operational ECMWF radiation scheme on 2 May 1989, corrects for most of the known deficiencies in the present clear-sky radiative parametrization. However, improvements of this new scheme are still possible. They are likely to come from

(i) a better knowledge of spectroscopic parameters, continuum, line shapes and intensities which should lead to a better representation of clear-sky fluxes;

(ii) in-situ quality measurements of the surface fluxes with high spectral resolution which should help validate the line-by-line models against which the new radiation scheme was calibrated; They will also help validate algorithms aiming at retrieving from satellite measurements the surface radiative budget, a model quantity that up to now has received only limited verification.

(iii) an extensive use of satellite data (such as ISCCP, ERBE), to document more precisely cloud fields and their radiative impact on various time and space scales. Together with the use of dedicated data sets of *in situ* measurements (FIRE Ci and Sc IFOs), it will improve the parametrization of clouds and cloud-radiation interaction which is the weakest part in radiation parametrization.

Acknowledgments:

I am indebted to various people for providing me with results of their detailed radiation transfer models: Results of the 4A longwave line-by-line model of Drs. Scott and Chédin have been available to me since 1984 and were very useful at various stages in the development and validation of the EC3 longwave scheme; Drs. Fels, Schwarzkopf, and Freidenreich provided the GFDL

longwave line-by-line model results used in the comparisons presented in the paper. B. Bonnel and Y Fouquart gave me a copy of their detailed shortwave narrow-band model. It is a pleasure to thank my colleagues of the Physical Aspects section of the ECMWF Research Department for the numerous discussions.

REFERENCES

Albrecht, B.A., V. Ramanathan, and B.A. Boville, 1986: The effects of cumulus moisture transport on the simulation of climate with a general circulation model. J. Atmos. Sci., 43, 2443-2462.

Arpe, K., 1988: Planetary-scale diabatic forcing errors in the ECMWF model. ECMWF Workshop on Diabatic Forcing, 30 Nov.-3 Dec. 1987. ECMWF, Reading, U.K., 103-150.

Betts, A.K., and W. Ridgway, 1988: Coupling of the radiative, convective, and surface fluxes over the Equatorial Pacific. J. Atmos. Sci., 45, 522-536.

Duvel, J.-Ph., and R.S. Kandel, 1985: Regional-scale diurnal variations of outgoing infrared radiation observed by METEOSAT. J. Climate Appl. Meteor., 24, 335-349.

Fels, S.B., and L.D. Kaplan, 1975: A test of the role of longwave radiative transfer in a general circulation model. J. Atmos. Sci., 32, 779-789.

Fouquart, Y., and B. Bonnel, 1980: Computations of solar heating of the earth's atmosphere: a new parameterization. Beitr. Phys. Atmosph., 53, 35-62.

Fouquart, Y., 1987: Radiative transfer in climate modeling. NATO Advanced Study Institute on Physically-Based Modeling and Simulation of Climate and Climatic Changes. Erice, Sicily, 11-23 May 1986. M.E. Schlesinger, Ed.,

Fouquart, Y., B. Bonnel, and V. Ramaswamy, 1989: Intercomparing shortwave radiation codes for climate studies. accepted for publication in J. Geophys. Res.

Frouin, R., C. Gautier, and J.-J. Morcrette, 1988: Downward longwave irradiance at the ocean surface from satellite data: Methodology and in situ validation. J. Geophys. Res., 93 C, 597-619.

Geleyn, J.-F., 1977: A comprehensive radiation scheme designed for fast computation. ECMWF Research Dept. Internal Report No. 8, 36 pp.

Geleyn, J.-F., and A. Hollingsworth, 1979: An economical analytical method for the computation of the interaction between scattering and line absorption of radiation. Beitr. Phys. Atmosph., 52, 1-16.

Geleyn, J.-F., 1981: Some diagnostics of the cloud/radiation interaction in ECMWF forecasting model. ECMWF Workshop on Radiation and Cloud-Radiation Interaction in Numerical Modelling, 15-17 Oct. 1980, ECMWF, Reading, U.K., 135-162.

Geleyn, J.-F., A. Hense, and H.-J. Preuss, 1982: A comparison of model generated radiation fields with satellite measurements. Beitr. Phys. Atmosph., 55, 253-286.

van Hoyt, D., 1976: The radiation and energy budgets of the Earth using both ground-based and satellite-derived values of total cloud cover. NOAA Tech. Report ERL 362-ARL4. U.S. Dept. of Commerce, Washington, D.C., 124 pp.

ICRCCM, The InterComparison of Radiation Codes in Climate Models, 1984: World Climate Programme Report 95, F.M. Luther and Y. Fouquart, Eds., Geneva, Switzerland.

Jaeger, L., 1976: Monatskarten des Niederschlags fur die Ganze Erde. Berichte des Deutschen Wetterdienstes, 139, 18.

Luther, F.M., R.G. Ellingson, Y. Fouquart, S. Fels, N.A. Scott, and W.J. Wiscombe, 1988: Intercomparison of radiation codes for climate models (ICRCCM). Longwave clear-sky results - A workshop summary. Bull. Amer. Meteor. Soc., 69, 40-48.

McClatchey, R.A., W.S. Benedict, S.A. Clough, D.E. Burch, R.F. Calfee, K. Fox, L.S. Rothman, and J.S. Garing, 1973: AFCRL atmospheric absorption line parameters compilation. AFCRL-TR-73-0096, Environ. Res. Paper No. 434, Bedford, Mass., 78 pp.

Morcrette, J.-J., and J.-F. Geleyn, 1985: On the influence of different radiation parameterizations on model-generated radiation fields. Quart.J.Roy.Meteor.Soc., 111, 565-585.

Morcrette, J.-J., and Y. Fouquart, 1985: On systematic errors in parametrized calculations of longwave radiation transfer. Quart.J.Roy.Meteor.Soc., 111, 691-708.

Morcrette, J.-J., and Y. Fouquart, 1986: The overlapping of cloud layers in shortwave radiation parameterizations. J. Atmos. Sci., 43, 321-328.

Morcrette, J.-J., L. Smith, and Y. Fouquart, 1986: Pressure and temperature dependence of the absorption in longwave radiation parameterizations. Beitr. Phys. Atmosph., 59, 455-469.

Morcrette, J.-J., 1988: Comparison of satellite-derived and model-generated diurnal cycles of cloudiness and brightness temperatures. Advances in Space Research, 8, (7), 175-179.

Morcrette, J.-J., and Y. Fouquart, 1989: Comparison of E.R.B.E. measurements with model-generated radiation fields. IRS'88: Current Problems in Atmospheric Radiation, J. Lenoble and J.-F. Geleyn, Eds., A. Deepak Publ., Hampton, Va. 332-334.

Morcrette, J.-J., 1989a: Impact of a change of radiation transfer scheme on the ECMWF model. ECMWF Technical Report N° 64, 52 pp.

Morcrette, J.-J., 1989b: Cloud-radiation diagnostics using ERBE and ISCCP data. ECMWF/EUMETSAT Workshop, 8-12 May 1989, ECMWF, Reading, in press.

Morcrette, J.-J., 1989c: Description of the radiation scheme in the ECMWF model. ECMWF Technical Memorandum N° 165, 26 pp.

Morcrette, J.-J., 1990: Radiation and cloud radiative properties in the ECMWF operational weather forecast model. J. Geophys. Res., in press.

NOAA, 19xx: Climate Diagnostics Bulletin, "month" "year". Available from NOAA/National Weather Service, National Meteorological Centre, Climate Analysis Center, Washington, D.C.

Ramanathan, V., E.J. Pitcher, R.C. Malone, and M.L. Blackmon, 1983: The response of a spectral general circulation model to refinements in radiative processes. J. Atmos. Sci., 40, 605-630.

Ramanathan, V., 1986: Atmospheric general circulation and its low frequency variance: Radiative influences. in: Short and Medium Range Weather Prediction. Collected papers presented at WMO/IUGG NWP Symposium, Tokyo, Japan, 4-8 Aug. 1986, ed. by T. Matsuno, Special Volume of the J. Meteor. Soc., 151-175.

Riehl, H., and J.S. Malkus, 1957: On the heat balance and maintenance of the circulation in the trades. Quart. J. Roy. Meteor. Soc., 83, 21-29.

Riehl, H., and J.J. Simpson, 1979: The heat balance of the equatorial trough zone: Revisited. Beitr. Phys. Atmosph., 52, 287-305.

Ritter, B., 1984: The impact of an alternative treatment of infrared radiation on the performance of the ECMWF forecast model. "IRS '84: Current problems in Atmospheric Radiation"., G. Fiocco, ed., A. Deepak Publ., Hampton, Va., 277-280.

Rossow, W.B., F. Mosher, E. Kinsella, A. Arking, M. Desbois, E. Harrison, P. Minnis, E. Ruprecht, G. Seze, C. Simmer, and E. Smith, 1985: ISCCP cloud algorithm intercomparison. J. Climate Appl. Meteor., 24, 877-903.

Rothman, L.S., 1981: AFGL atmospheric absorption line parameters compilation: 1980 version. Appl. Opt., 20, 791-795.

Schiffer, R.A., and W.B. Rossow, 1983: The International Satellite Cloud Climatology Project (ISCCP): The first project of the World Climate Research Programme. Bull. Amer. Meteor. Soc., 76, 779-784.

Schiffer, R.A., and W.B. Rossow, 1985: ISCCP Global Radiance Data Set: A new resource for climate research. Bull. Amer. Meteor. Soc., 66, 1498-1505.

Scott, N.A., and A. Chedin, 1981: A fast line-by-line method for atmospheric absorption computations: The Automatized Atmospheric Absorption Atlas. J. Appl. Meteor., 20, 802-812.

Selby, J.E.A., and R.A. McClatchey, 1975: Atmospheric Transmittance from 0.25 to 28.5 microns: Computer code LOWTRAN 3, AFCRL-75-0255, Environment Res. Paper 513, Bedford, Mass., 75 pp.

Slingo, A., and J.M. Slingo, 1988: The response of a general circulation model to cloud longwave radiative forcing: I. Introduction and initial experiments. Quart. J. Roy. Meteor. Soc., 114, 1027-1062.

Slingo, J.M., 1982: A study of the earth's radiation budget using a general circulation model. Quart. J. Roy. Meteor. Soc., 108, 379-405.

Slingo, J.M., 1987: The development and verification of a cloud prediction scheme for the ECMWF model. Quart. J. Roy. Meteor. Soc., 113, 899-928.

Slingo, J.M., U.C. Mohanty, M. Tiedtke, and R.P. Pearce, 1988: Prediction of the 1979 Summer monsoon onset with modified parameterization schemes. Mon. Wea. Rev., 116, 328-346.

Slingo, J.M., and B. Ritter, 1985: Cloud prediction in the ECMWF model. ECMWF Tech. Report No. 46, ECMWF, Reading, U.K.

Stephens, G.L., 1978: Radiative properties of extended water clouds. Parts I and II., J. Atmos. Sci., 35, 2111-2122, 2123-2132.

Tanre, D., J.-F. Geleyn, and J.M. Slingo, 1984: First results of the introduction of an advanced aerosol-radiation interaction in the ECMWF low resolution global model. Aerosols and Their Climatic Effects. H.E. Gerber and A. Deepak, Eds., A. Deepak Publ., Hampton, Va., 133-177.

Tiedtke, M., J.-F. Geleyn, A. Hollingsworth, and J.-F. Louis, 1979: ECMWF model: Parameterization of subgrid-scale processes. ECMWF Tech. Report No. 10, ECMWF, Reading, U.K.

Tiedtke, M., W.A. Heckley, and J. Slingo, 1988: Tropical forecasts at ECMWF: On the influence of physical parameterization on the mean structure of forecast and analyses. Quart. J. Roy. Meteor. Soc.,

Tiedtke, M., and M.J. Miller, 1988: Convection and i ts parameterization - Recent progress. ECMWF Research Dept. Tech. Memo. No. 147, 39 pp., ECMWF, Reading, U.K.

Verstraete, M.M., and R.E. Dickinson, 1986: Modeling surface processes in atmospheric general circulation models. Annal. Geophys., B 4, 357-364.

Vigroux, E., 1953: Contribution à l'étude experimentale de l'absorption de l'ozone. Annales Phys., 8, 709.

Wiscombe, W.J., and J.W. Evans, 1977: Exponential sum fitting of radiative transmission functions. J. Comput. Phys., 24, 416-444.

W.M.O., 1984: The Intercomparison of Radiation Codes in Climate Models (ICRCCM), Longwave Clear-Sky Calculations. Frascati, Italy, 15-18 Aug. 1984, World Climate Programme Report WCP-93, Geneva, Switzerland, 37 pp.

WMO-ICSU, 1985: International Satellite Cloud Climatology Project (ISCCP): Description of reduced resolution radiance data. WMO/TD-No. 58, Geneva, Switzerland, 132 pp.

Zdunkowski, W.G., G.J. Korb, and B.C. Nielsen, 1967: Prediction and maintenance of a radiation fog. U.S. Army Electronics Command Report Contract DAAB07-67-c-0049.